IMPACT PRESSURE AND TOTAL TEMPERATURE INTERPRETATION AT HYPERSONIC MACH NUMBERS

Thesis by

Norwald R. Quiel

Lieutenant, U. S. Navy

In Partial Fulfillment of the Requirements

For the Degree of

Aeronautical Engineer

California Institute of Technology

Pasadena, California

1954

ACKNOWLEDGMENTS

The author wishes to express his appreciation to Dr. H. T. Nagamatsu for his continued guidance and encouragement throughout this investigation.

Sincere thanks are extended to the staff of the GALCIT Hypersonic Wind Tunnel for their complete cooperation, to the members of the GALCIT Machine Shop who skilfully fabricated the test equipment, and finally, to Mrs. H. Van Gieson, Miss F. Scheinis, and Miss N. Waldron for their aid in the preparation of the final manuscript.

ABSTRACT

An experimental investigation was undertaken at a nominal Mach number of 5.6 in the GALCIT Hypersonic Wind Tunnel, Leg No. 1. The first phase was an investigation of the viscous effects on measured impact pressures. The second was an investigation of the temperature recovery characteristics of a singly shielded total-temperature probe.

Experimental results are presented for a straight, sharp-lipped, cylindrical, impact-pressure probe and for a flattened-end probe. Impact-pressure data were obtained for a Reynolds number range from 425 to 8,000, where the Reynolds number was based on free stream conditions and the impact probe outside diameter. The data show that the Rayleigh equation requires corrections for viscous effects at Reynolds numbers less than 6,000 for the circular sharp-lipped probe and less than 4,000 for the flattened-end probe. The viscous effects increase with decreasing Reynolds numbers. At a Reynolds number of 425, the measured impact pressure is approximately 2.5 per cent lower than that predicted by the Rayleigh equation. It was concluded that the viscous effects were dependent on Mach number as well as Reynolds number.

Temperature recovery factors for the total-temperature probe were obtained throughout a Reynolds number range from 30,800 to 213,000, where the Reynolds number was based on the probe entrance outside diameter and the free stream conditions. An analysis of suitable parameters with which to present the data is included together with the experimental data. For a limited range of total temperatures, a single temperature recovery calibration curve was obtained when the Reynolds number was used as a parameter. The data show that the temperature recovery factor of the total temperature probe decreases with decreasing Reynolds numbers.

TABLE OF CONTENTS

PART		PAGE
	Acknowledgments	ii
	Abstract	iii
	Table of Contents	iv
	Nomenclature	vi
I.	Introduction	1
II.	Equipment and Procedure	7
	A. Wind Tunnel Description	7
	B. Model Description	8
	1. Impact-Pressure Probe Rake	8
	2. Stagnation-Temperature Probes	8
	3. Static-Pressure Probe	9
	C. Instrumentation	10
	1. Pressure Measurements	10
	2. Temperature Measurements	10
	D. Test Procedure	10
	1. Impact-Pressure Runs	10
	2. Total-Temperature Runs	12
III.	Reduction and Analysis of Data	13
	A. Impact-Pressure Correction Technique	13
	B. Determination of Flow Parameters	13
	1. Mach Number	13
	2. Reynolds Number	14

3. Knudsen Number 16

4. Nusselt Number 17

C. Temperature Recovery Factor Determination 19

IV. Experimental Results and Discussion 21

A. Impact Pressure Measurements 21

1. Experimental Results 21

2. Consideration of the Methods of Data Presentation 22

3. Comparison with Previous Experimental Investigations and Theory 23

B. Total-Temperature Probe Calibration 25

1. Initial Calibration for Comparison of Probes A and B 25

2. Extended Calibration of Probe A 26

3. Suitability of Parameters for Presenting Temperature Recovery Factor Calibrations 27

4. Comparison with a Previous Experimental Investigation 28

V. Conclusions and Recommendations 30

References 31

Appendix A -- Temperature Error at a Thermocouple Junction Due to Conduction in the Thermocouple Wires 33

Appendix B -- Accuracy Analysis of Experimental Data 37

List of Figures 39

Figures 41

NOMENCLATURE

a	speed of sound, ft./sec.
A	area, sq. ft.
A^*	area of a sonic throat, sq. ft.
c_p	specific heat at constant pressure, Btu/(lb.)(deg. F)
d	probe outside diameter, inches
d_i	probe inside diameter, inches
h	heat transfer coefficient, Btu/(sq. ft.)(deg. F)(sec.)
h	characteristic outside dimension for flattened probes, inches
J	constant conversion factor = 778 ft. lb./Btu
k	thermal conductivity, Btu/(ft.)(deg. F)(sec.)
ℓ	mean molecular free path length, inches
M	Mach number, u/a, dimensionless
M_p	Mach number inside temperature probe = constant
Nu	Nusselt number, hd/k, dimensionless
Nu^*	defined by $Nu\ k_g / \sqrt{M_p}\ k_w$, dimensionless
p	pressure, lbs./sq. in.
Pr	Prandtl number, $\mu\ c_p/k$, dimensionless
Q	heat flux, Btu/sec.
r	temperature recovery factor, dimensionless
R	gas constant for air = 1715 sq. ft./(sec.^{2})(deg. F)
Re	Reynolds number, $\rho\ ud/\mu$, dimensionless
Re^*	Reynolds number evaluated at total temperature
T	absolute temperature, deg. R
u	local velocity, ft./sec.

$\bar{v}$ mean molecular velocity, ft./sec.

x variable length, ft.

γ ratio of specific heats, c_p/c_v, dimensionless

λ a length of thermocouple wire, inches

μ absolute viscosity, lb. sec./sq. ft.

ρ mass density, lb. $sec.^2/ft.^4$

Subscripts

$( )_g$ refers to gas conditions

$( )_o$ stagnation or reservoir conditions

$( )_w$ pertaining to the thermocouple wire

Superscripts

$( )'$ conditions after normal shock, for an inviscid fluid

$( )''$ stagnation conditions as read by impact-pressure probe

I. INTRODUCTION

Velocities of fluid streams which are much greater than the local acoustic velocity are commonly referred to as "hypersonic" velocities. For the sake of definiteness, the hypersonic regime is arbitrarily considered in this report as the Mach number range above 5.

Recent developments in guided missiles and rockets, which are designed to travel at hypersonic Mach numbers and extreme altitudes, have necessitated obtaining basic aerodynamic data in hypersonic wind tunnels. The difficulty in accurately obtaining local fluid stream data such as Mach number, Reynolds number, etc., is much more severe in a rarified hypersonic air stream than in supersonic or subsonic flow streams of higher density. The problem specifically treated in this experimental investigation is that of interpreting and calibrating impact-pressure measurements and total-temperature measurements in a hypersonic flow.

For measurements of impact pressures in a moving fluid field a total head tube is conventionally used. The tube is aligned with its axis parallel to the flow, and the fluid stream is brought to rest at the open end of the tube. The pressure at the open end of the tube is then determined by a suitable pressure sensing system. Impact pressure interpretation at low densities and in subsonic and supersonic flows has been the subject of several theoretical and experimental investigations (Refs. 1 to 8).

For supersonic continuum flow of a compressible, non-viscous fluid the familiar Rayleigh formula (Cf. Ref. 9, p. 77) provides a method of relating impact pressure to the static pressure and Mach number.

Application of the Rayleigh pitot-tube equation implies that in the fluid stream behind a normal shock only the inertia forces are significant; consequently use of this equation becomes increasingly inaccurate for conditions in which the viscous forces become appreciable compared to the inertia forces. A criterion for this viscous force effect is the Reynolds number of the flow based on a suitable characteristic dimension.

For the case of a continuum, supersonic, compressible, viscous flow, (i.e., low Re) theoretical corrections have been applied to the Rayleigh equation (Refs. 4 and 5) for selected probe geometries.

For extremely low density fluid flow in which continuum flow analyses no longer are valid, the theoretical ordinary gas dynamics predictions for the impact pressures must be set aside. The general field of rarefied gas dynamics has been discussed by Tsien in Ref. 10. A useful criterion for estimating the low density effects is the molecular mean free path length, which can be defined as the average distance between molecular collisions. The ratio of the mean molecular free path to a characteristic dimension of a body immersed in a fluid stream, $\ell/d \sim M/Re$, is a significant parameter for estimating the magnitude of the low density effect.

The magnitude of the ratio ℓ/d for which the methods of continuum flow mechanics are inadequate is not well defined. On the basis of considerations of experimental data obtained by Kane and Maslach (Ref. 2), it appears that continuum fluid dynamics theory requires corrections for ℓ/d values greater than about .015.

When the molecular mean free paths are large, of the approximate order of 10, compared to body dimensions, a fully developed molecular flow exists (Cf. Ref. 10). In this case, the collisions of a molecule

with the body in the stream are much more frequent than collisions with other molecules, and the methods of kinetic theory of gases must be used to predict impact pressures.

With increasing molecular mean free path, the normal shock wave becomes thicker and less well defined and may not even exist as such for a fully developed free molecular flow. Therefore, a modified Rayleigh formula which omits the shock wave entirely might be of considerable interest at low densities. Chambre and Schaaf (Ref. 6) have derived an equation predicting the impact pressure based on consideration of kinetic theory for fully developed molecular flow.

In the transition region between continuum and fully developed molecular flow, no theory predicting the impact pressures in a moving stream exists at present. For this transition region Kane and Maslach (Ref. 2) have made an experimental investigation of impact pressures near the estimated continuum limit, ℓ/d from .138 to .0123 and over a Mach number range 2.3 to 3.6 and Reynolds number range of 25 to 804. Sherman (Ref. 1) has also made an experimental investigation of impact pressures near the estimated continuum limit, ℓ/d = .003 to .11, Mach number range of 1.7 to 4.0, and Reynolds number range of 15 to 800.

The results of both of these experimental investigations showed viscous corrections at very low Reynolds numbers, which yielded impact pressures higher than those which would be computed from Rayleigh's formula. In addition, Ref. 1 indicates a region at slightly higher Reynolds numbers where the impact pressure was less than that predicted by non-viscous theory.

As a conclusion to Ref. 2, a need was expressed for further experimental tests at higher Mach numbers. The impact-pressure phase of this investigation involves experiments designed to provide the extended Mach number range and to include a comparison of two probe geometries.

Because of practical considerations and limited time, this investigation was restricted to a nominal Mach number of 5.6 and a minimum Reynolds number of the order of 400 based on impact probe outside diameter and free stream conditions. The emphasis on this phase of investigation was to obtain experimental data, at hypersonic Mach numbers and low Reynolds numbers, on the variation of experimental impact -- pressure measurements from those predicted by Rayleigh's equation. In addition, it was desired to substantiate the general trends in this variation as determined by previous investigators at lower Mach numbers.

The design and calibration of total-temperature probes for use at hypersonic velocities have been the subject of relatively few experimental investigations (Cf. Ref. 11). For subsonic and supersonic velocities the design and calibration of total-temperature probes have been investigated in Refs. 12 and 13.

The design of a total-temperature probe to give a relatively constant calibration for a certain range of test conditions is largely a qualitative process involving the selection of materials and dimensions which will fit the test conditions. In order to approach the optimum design of a total-temperature probe for use at hypersonic velocities, a considerable amount of theoretical study and experimental investigation is required. E. M. Winkler of the Naval Ordnance Laboratory has made rather extensive design and calibration studies for total-temperature

probes at hypersonic velocities and over a considerable range of Reynolds numbers.

The most useful method of presenting total-temperature calibration data is by means of a single calibration curve that would be valid for all flow conditions. The choice of a parameter of the fluid flow which will produce a single curve is not immediately obvious. The results of previous temperature probe calibrations have conventionally been presented with either Mach number or Reynolds number as the variable parameter. However, in the hypersonic range use of one of these parameters as the variable results in families of calibration curves for constant values of the other parameter.

The dependence of temperature recovery on Nusselt number is considered in Ref. 11. The Nusselt number, based on thermocouple wire diameter and conditions inside the probe, was calculated, and this number was then multiplied by the ratio of gas thermal conductivity to mean thermal conductivity of the thermocouple wires. This parameter is a measure of the heat transfer balance at the thermocouple junction as indicated in the analysis contained in Appendix A. In Ref. 11, temperature recovery factor for a given probe was plotted versus this parameter, and the resulting plot produced a single curve which was valid for a considerable range of Mach numbers, Reynolds numbers, and stagnation temperatures of the flow.

The design of a new type total-temperature probe was not considered in this investigation. The scope of this investigation was simply to construct a temperature probe based on existing designs that had proved successful and to calibrate this total-temperature probe at

a nominal Mach number of 5.6 over a range of free stream Reynolds numbers. Two total-temperature probes based on designs suggested in Ref. 11 were adapted for use in this program.

The emphasis in this phase of the investigation was on obtaining data over the greatest possible range of Reynolds numbers and total temperatures and on converting these data to obtain calibration curves for temperature recovery factors so that these temperature probes could be used in further experimental work. It should be noted that the calibration curves are limited to use with the two temperature probes tested.

This experimental project was conducted in the GALCIT 5 x 5 inch Hypersonic Wind Tunnel Leg No. 1 in cooperation with LT J. C. Graves, U. S. Navy, and under the supervision of Dr. H. T. Nagamatsu.

II. EQUIPMENT AND PROCEDURE

A. Wind Tunnel Description

The GALCIT 5 x 5 inch Hypersonic Wind Tunnel (Leg No. 1) was used for these tests. It is of the continuously-operating, closed-return type and is operated by a compressor plant consisting of sixteen compressors driven by seven electric motors. The thirteen compressors in the first five compression stages are Fuller rotary compressors, while the final two stages consist of three reciprocating compressors. A system of valves and interconnecting piping permits the selection of a wide variety of plant compression ratios and mass flows. These valves, as well as the compressors, are operated remotely from a master control panel (Cf. Fig. 1). A schematic diagram of the wind tunnel installation is shown in Fig. 2.

The Leg No. 1 test section with fixed nozzle blocks designed for a nominal Mach number of 6 was used for these tests. The nozzle blocks were designed by the Foelsch analytical method with correction applied for the estimated boundary layer growth. Static orifices were provided at one-inch intervals in both nozzle blocks to permit a check to be made with the original nozzle calibration.

The Leg No. 1 air heating system employs superheated steam in a multiple pass heat exchanger and is capable of producing a maximum stagnation temperature of about 300°F at a reservoir pressure of 94 psia, and 230°F at atmospheric reservoir pressure.

The water content in the air was kept well below 100 parts per million (by weight) by passing it through a tank containing approxi-

mately 2000 pounds of silica gel. Oil was removed by Cyclone separators after each compression stage and, in addition, by finely-divided activated carbon canisters, porous carbon filter blocks, and a Mine Safety Appliances "Ultra-Aire Space Filter".

B. Model Description

1. Impact-Pressure Probe Rake

Six stainless steel probes, of varying diameter, were mounted on a 2 inch x $2\frac{1}{2}$ inch stainless steel, wedge-shaped rake as shown in Fig. 3. The lead-in tubes, also of stainless steel, were completely enclosed within the wedge and its 5/16 inch diameter support rod. With the use of the externally-operated model control system in the tunnel test section, the rake could be moved vertically so as to bring each probe into the tunnel center line.

Two probe-end geometries were used. The Type I probes were sharp-lipped and circular-ended with outside diameters varying from 0.016 inch to 0.25 inch. The Type II probes were made by flattening the ends of round tubes so that the ratio of outside height to outside width was one-third. Sizes of probe-end outside heights ranged from 0.014 inch to 0.109 inch. Figure 4 shows a schematic sketch of these two probe geometries.

2. Stagnation-Temperature Probes

Two stagnation-temperature probes were constructed, both essentially similar to the design given in Ref. 11 but differing from each other in outside diameter of the probe entrance and thermocouple wire

diameter. Both probes consisted of a single platinum-coated quartz shield cemented to a stainless steel holder with a high-temperature ceramic cement. To replace continuously the air inside the probe, a single vent hole was provided in the shield aft of the thermocouple so that the vent-area to entrance-area ratio was approximately 1:5. Experimental data in Ref. 11 indicate that this area ratio is an optimum value. Iron-constantan thermocouples were cemented into a quartz support, which in turn was sealed into the stainless steel holder.

Probe A had an entrance outside diameter of 0.10 inch, and B. and S. gage 30 (.01 inch diameter) thermocouple wire was used, while the outside diameter of the entrance of Probe B was .063 inch, and 0.012 inch diameter thermocouple wire was used. Fig. 5 gives a schematic sketch of these probes, and Fig. 6 shows the probe support on which the probes were mounted for placement in the tunnel. It should be noted that this latter probe support also included an impact-pressure probe and a static-pressure probe, in addition to the temperature probe, so that flow conditions in the tunnel test section could be measured readily. Each probe could be positioned in turn on the tunnel center line by means of the model support control.

3. Static-Pressure Probe

The static-pressure probe was constructed of 0.083 inch outside diameter stainless steel tubing with a solid 10 degree conical nose. Three static orifices spaced uniformly around the tube circumference were located 30 diameters downstream from the nose.

C. Instrumentation

1. Pressure Measurements

The reservoir pressure was measured with a Tate-Emery nitrogen-balanced gage and controlled within ± 0.04 psi by a Minneapolis-Honeywell-Brown circular chart controller. All static and impact pressures were measured on a silicone fluid, vacuum-referenced manometer (Fig. 1). With the latter, pressures could be easily read to the closest 0.1 cm and estimated to 0.01 cm of silicone. This estimate is approximately equivalent to 0.07 microns of mercury.

2. Temperature Measurements

The tunnel stagnation temperature was measured by an iron-constantan, shielded thermocouple located one inch upstream from the nozzle throat and was recorded and controlled by a Minneapolis-Honeywell-Brown circular chart controller to within ±2°F. The thermocouples in the stagnation-temperature test probes were differentially connected with the reservoir thermocouple to a Leeds and Northrup slide-wire potentiometer, as shown schematically in Fig. 7.

D. Test Procedure

1. Impact-Pressure Runs

Prior to the installation of the probe rake in the test section, an axial static pressure survey was conducted on the tunnel center line to locate a region of uniform pressure. A point 19.7 inches aft of the throat was selected, and the impact-pressure probe ends were aligned

accordingly. In addition, a vertical total-head survey was made at this position with results as shown in Fig. 8.

After the probe rake was installed and connected to the manometer, each complete system was carefully leak-checked. With the tunnel operating at a specified reservoir condition, each of the six different-sized probes on the rake was in turn placed at the test section center line, and its pressure measured on the silicone manometer. This positioning was accomplished with the vertical-actuating model control system, which was externally operated. In addition to counter readings on the vertical supports, it was found desirable to use the schlieren system and a fixed grid network placed on the glass port to check the center line positioning. The cycle was repeated until a determination of the reproducibility of results was completed.

Since it was desired to obtain the lowest possible Reynolds number (and consequently, the lowest air density) in the test section, the stagnation conditions of minimum possible stagnation pressure (p_o) with the corresponding maximum total temperature (T_o) were selected for one run. In addition, several runs at slightly lower T_o's and higher p_o's were made.

The actual reservoir temperature and pressure combinations used were as follows:

p_o(psia)	T_o(^oF)	Remarks
14.7	230	one-phase flow
14.7	221	one-phase flow
14.7	210	one-phase flow
30.7	242	one-phase flow

A schlieren picture was taken of the flow around the probe rake to determine if any shock wave interference existed from one probe to another. Referring to Fig. 9, it is seen that the strongest shock wave, created by the largest probe, does not intersect the adjacent probe until it is many diameters downstream.

2. Total-Temperature Runs

The total-temperature probe was mounted in the tunnel on a support which also included a total-pressure probe and a static-pressure probe as shown in Fig. 6. The latter two probes were connected to the manometer system and then carefully leak-tested. The leads from the test thermocouple were differentially connected with the reservoir thermocouple to the potentiometer. Thus, the e.m.f. read on the potentiometer was proportional to the temperature difference between T_o and the temperature sensed by the test probe, T_o'.

For each calibration run, the reservoir temperature was held fixed and the reservoir pressure varied throughout its possible range. At each flow setting the total pressure, static pressure, and e.m.f. were recorded.

III. REDUCTION AND ANALYSIS OF DATA

A. Impact-Pressure Correction Technique

In order to determine a viscous correction, it is first necessary to find the value which the impact pressure would have if the flow were essentially inviscid. This value could be determined if an impact probe were used which was sufficiently large that the viscous effects were no longer detectable. However, it was not known intuitively whether the Reynolds number of the largest probe on the probe rake tested was large enough to be free of viscous effects. Consequently, some additional analysis was necessary.

A method of attack which proved quite satisfactory in Ref. 1 was employed. This technique consisted of plotting the measured impact pressures against the inverse of impact-probe diameters for the six different-sized probes tested and extrapolating a curve through the resulting points to $1/d = 0$. The value of the pressure intercept at this point was considered to be that corresponding to the impact pressure in an inviscid fluid.

This process of letting $1/d$ approach zero was considered equivalent to letting the Reynolds number approach infinity, all other factors in Re having been held constant. Typical plots of data involving this process are shown in Fig. 10.

B. Determination of Flow Parameters

1. Mach Number

With the measured impact pressure, corrected for viscous effects as explained previously, plus the measured static pressure, the free

stream Mach number was calculated using Rayleigh's well-known supersonic pitot tube equation. In the instance where the static pressure was measured during a run subsequent to a series of impact-pressure runs, the reproducibility of flow conditions was checked by means of a reference impact-pressure probe.

The subsonic Mach number of the flow within the total-temperature probes was calculated simply from the area ratio of the shield inside diameter to the vent. Since the pressure ratio at the vent, p/p_o', is well below the critical value, a sonic throat exists in the vent passage. Thus, for a given probe geometry, the Mach number of the flow within the probe is essentially independent of free stream flow conditions.

2. Reynolds Number

The Reynolds number per inch based on undisturbed free stream conditions was calculated for each flow setting. The corresponding Reynolds number for each impact probe based on the outside diameter was then determined. The measured free stream pressure, the stagnation temperature, and the corresponding value of the Mach number were used to compute the Reynolds number.

By definition we can write

$$Re = \frac{\rho u d}{\mu} = \frac{\rho M a d}{\mu} \tag{1}$$

The assumption of the perfect gas law gives $\rho = p/RT$, and the sonic velocity, a, is given by $a = \sqrt{\gamma RT}$. Substituting for ρ and a in Eq. (1) we obtain

$$Re = \frac{M \sqrt{\gamma RT}\, pd}{\mu RT} \tag{2}$$

which reduces to

$$Re = 0.343 \frac{p M d}{\mu \sqrt{T}} \tag{3}$$

for $\gamma = 1.4$ and $R = 1715$ ft./sec.^{2} $^\circ$R. The units of p, d, u, and T are given in the list of symbols.

By assuming adiabatic flow the free stream temperature, T, was then obtained from the equation

$$T = \frac{T_o}{1 + \frac{\gamma - 1}{2} M^2} \tag{4}$$

A plot of this equation given in Ref. 14 was used.

The corresponding value for the viscosity of air was obtained from a plot of the Keyes' equation for viscosity. Ref. 15 indicates that for air at very low temperatures Keyes' equation is more appropriate than the familiar Southerland's equation for viscosity. For air, Keyes' equation becomes

$$\mu \text{(slugs/ft. sec.)} = 2.316 \times 10^{-10} \frac{\sqrt{T}}{1 + \frac{219.8}{T} 10^{-9/T}} \tag{5}$$

At higher temperatures (above 500°R) the viscosity for air was obtained from curves based on Southerland's equation given in Ref. 16.

Thus, all the properties used to characterize the air stream have been those of the undisturbed free stream. It was also desired to obtain a set of reference properties based on conditions behind a normal shock wave. The change in properties of a free stream passing through a normal shock wave was calculated by the use of curves of normal shock wave functions given in Ref. 14.

3. Knudsen Number

The mean molecular free path lengths for the undisturbed free stream and for flow conditions after a normal shock wave were calculated. For each probe the corresponding Knudsen numbers were determined. From Kinetic theory, Chapman gives (Ref. 17)

$$\mu = 0.499\, \rho\, \bar{v}\, \ell \tag{6}$$

where $\bar{v}$ is the mean molecular speed and ℓ is the mean molecular free path length. Results from kinetic theory also connect $\bar{v}$ with the velocity of sound, a, by

$$\bar{v} = \sqrt{\frac{8}{\pi \gamma}}\ a \tag{7}$$

where γ is the ratio of specific heats. Combining Eqs. (6) and (7) yields

$$\ell = \frac{0.499\ \mu}{\rho\, a}\ \sqrt{\frac{\pi \gamma}{8}} \tag{8}$$

Noting that $\mu/\rho a = d\ M/Re$ and using $\gamma = 1.4$ for air, Eq. (8) becomes

$$\ell = 1.49\ (M/Re)\ d \tag{9}$$

The Knudsen number is now expressed as a function of Reynolds number and Mach number:

$$\ell/d = 1.49\ (M/Re) \tag{10}$$

4. Nusselt Number

The Nusselt number considered here involves the rate of heat transfer between the air flow and the thermocouple wire. It is defined in general by

$$Nu = \frac{h\, d_w}{k_g} \tag{11}$$

where h = heat transfer coefficient

k_g = gas thermal conductivity

d_w = thermocouple wire diameter

Moreover, for flow in which heat transfer is taking place we may write

$$Nu = f_1(M, Re, Pr) \tag{12}$$

where Pr is the Prandtl number for air and may be considered as remaining constant. Now, if we determine the Reynolds number, Re^*, based on an evaluation of gas density and viscosity at total temperature rather than at static temperature, then

$$Re^* = g(Re, M) \tag{13}$$

and so

$$Nu = f_2(Re^*) \tag{14}$$

In Ref. 18, a semi-empirical equation has been determined for this relation, namely,

$$Nu = 0.431 \sqrt{Re^*} \tag{15}$$

With this equation the Nusselt number of the flow inside the total-

temperature probe (based on thermocouple wire diameter) is easily calculated from measured quantities as follows:

$$Re^* = \frac{\rho_o V_p d_w}{\mu_o} = \frac{0.343\, p_o' M_p d_w \sqrt{T}}{T_o \mu_o}$$

$$Re^* = \frac{0.343\, p_o' M_p d_w}{\sqrt{T_o}\ \mu_o (1 + 0.2 M_p^2)^{\frac{3}{2}}} \tag{16}$$

where

p_o' = impact pressure in lbs./in.^{2}

μ_o = $f(T_o)$ = gas viscosity in lbs./ft.^{2}-sec.

d_w = thermocouple wire diameter in inches

M_p = Mach number inside probe

For the given probe geometries considered, there exists the problem of determining the proper area ratio to use in calculating M_p. However, considering the entrance area, where M_p is even greater than it is at the thermocouple wire, we find

$$A/A^* = 5 \quad , \quad M_p = 0.177$$

Thus, the variation of the denominator of Eq. (16) with M_p is negligible, and we can write

$$\frac{Re^*}{M_p} = \frac{0.343\, d_w\, p_o'}{\sqrt{T_o}\ \mu_o} \tag{17}$$

where the indefiniteness of calculating the constant M_p is eliminated by including it with the parameter Re^*.

From experimental results in Ref. 11 and an analysis of heat transfer balance in the thermocouple wire contained in Appendix A, it appears that the parameter Nu k_g/k_w is significant for the investigation of the temperature recovery factor. Accordingly, a parameter Nu^* is defined

$$Nu^* = \frac{Nu\, k_g}{\sqrt{M_p}\; k_w} \tag{18}$$

Using Eqs. (15) and (17), this may be written

$$Nu^* = \frac{0.252\, d_w^{\frac{1}{2}}\, p_o'^{\frac{1}{2}}\, k_g}{T_o^{\frac{1}{4}}\, \mu_o^{\frac{1}{2}}\, k_w} \tag{19}$$

For the thermocouple, k_w is a constant and may be considered as the mean of the two values for iron and constantan. However, k_g varies with the changing conditions of the gas. In Ref. 18, a suggested formula for calculating k_g is

$$k_g = 3.03 \times 10^{-8}\, T^{0.78} \tag{20}$$

Thus, for a given probe geometry, Nu^* is dependent only on the local reservoir conditions; and for any given run at a constant T_o, Nu^* is a function only of impact pressure, p_o'.

C. Temperature Recovery Factor Determination

In order to calibrate a total-temperature probe for future application, some measure of its ability to convert all of the kinetic energy of an air stream into heat energy must be obtained. For this

purpose a temperature "recovery factor" is commonly defined as

$$r = \frac{T_o' - T}{T_o - T} \tag{21}$$

where T_o' is the temperature sensed by the probe.

Since it was desired to measure as accurately as possible the small difference between T_o and T_o', the probe thermocouple was differentially connected with the reservoir thermocouple, as shown in Fig. 7. In this manner, the e.m.f. read on the potentiometer was proportional to the difference, $T_o - T_o'$. Using the thermocouple temperature-millivolt equivalent, the temperature difference was converted to degrees Fahrenheit.

With the recording of reservoir temperature, T_o, and subsequent calculation of the stream temperature, T, using the adiabatic energy equation, all information for determining recovery factor was available.

IV. EXPERIMENTAL RESULTS AND DISCUSSION

A. Impact Pressure Measurements

1. Experimental Results

Impact pressure data were obtained at a nominal Mach number 5.6 for impact pressure probe Types I and II as described in Section II.

The range of test conditions are summarized as follows:

$$M = 5.3 \text{ to } 5.6$$

$$Re = 425 \text{ to } 8{,}000$$

The primary results of this phase of the investigation are shown in Figs. 11-16 which show corrections to be applied to measured impact pressures. Two different parameters based on free stream conditions were used to present the corrections which are given as the ratio of measured impact pressure, p_o'', to the ideal non-viscous impact pressure, p_o'. In addition to the parameters based on free stream conditions, the impact pressure ratios obtained for impact pressure probe Type I are presented in Figs. 13 and 14, as a function of the same parameter based on flow conditions behind a normal shock.

The results of the experiments show that the Rayleigh formula requires corrections for viscous effects when the Reynolds number based on free stream conditions is less than 6,000 for probe Type I and less than 4,000 for probe Type II. However, the correction is small for the range of Reynolds numbers obtained in this investigation. The maximum deviation of the measured impact pressure, obtained at the low pressure limit of the experimental equipment, was 2.5 per cent. The deviations of the measured impact pressures from the ideal impact

pressures were negative in sense that the measured impact pressure was less than the ideal non-viscous impact pressure (i.e., $p_o''/p_o' < 1$).

It should be noted here that the specific impact-pressure correction data presented are valid only for the range of Mach numbers used to obtain the data and for the particular types of probes considered.

2. Consideration of the Methods of Data Presentation

Presentation of the data versus a parameter based on free stream conditions is most desirable from the viewpoint of practical application of the data to correction of measured impact pressures. The deviations of measured impact pressure from that predicted by the Rayleigh equation are caused by viscous and low density effects. Consequently, the Reynolds number and the Knudsen number based on free stream conditions and the impact probe diameter were chosen as significant parameters.

It is not to be expected that the calibration curves, obtained for measured impact-pressure correction versus parameters based on free stream conditions, are independent of Mach number. However, over the limited range of Mach numbers encountered in this investigation the dependence of the impact-pressure calibration curves on Mach number was not apparent.

Use of flow parameters based on stream conditions behind a normal shock permits comparison with experimental results for impact-pressure corrections in subsonic flows. For a more detailed study of the data and correlation with theory, the most useful presentation is a plot of measured impact-pressure correction versus parameters based on stream conditions behind a normal shock (Cf. Figs. 13 and 14).

3. Comparison with Previous Experimental Investigations and Theory

Only a qualitative comparison with previous investigations can be made as the present investigation was conducted at considerably higher Mach numbers than any previous experimental work. The most significant difference in results obtained in this investigation as compared with results of similar investigations is that the viscous effects on impact-pressure measurements become apparent at much larger Reynolds numbers for the higher Mach numbers encountered in this investigation.

The results shown in Ref. 1 for a probe of Type I at a nominal Mach number of 2.5 show increasing viscous effects on measured impact pressure with decreasing Reynolds numbers, beginning at Reynolds numbers of 150 to 200. The present results at nominal Mach number 5.6 show viscous effects for Reynolds numbers less than 6,000. Qualitatively, the results of this investigation are in agreement with experimental results shown in Ref. 1 for an impact-pressure probe of Type I. The results of Ref. 1 show measured impact pressures less than the ideal over the range of Reynolds numbers from 30 to 200. For Reynolds numbers below 30 the data of Ref. 1 show measured impact pressures greater than the ideal.

Experimental results for a source shaped probe (Refs. 1 and 2) show consistently increasing p_o''/p_o' with decreasing Reynolds number. It appears that the source-shaped probe has somewhat different viscous characteristics than those of Types I or II.

It is possible that the curve shown in Fig. 11 might tend to swing up to values of p_o''/p_o' greater than one if data at the lower

Reynolds numbers were included. It should be noted here that the minimum value of the ratio p_o''/p_o' observed in this investigation was lower by approximately 2 per cent than the values of p_o''/p_o' shown in Ref. 1 for a probe of Type I.

An attempt to correlate directly p_o''/p_o' with $\ell/d \sim M/Re$ fails when a comparison is made with the results of Ref. 1. For a nominal Mach number of 2.5 the viscous effects become apparent for values of ℓ/d less than .0196 as calculated from the data contained in Ref. 1. As shown in Fig. 12 the viscous effects at a nominal Mach number of 5.6 become apparent for ℓ/d less than .001. The comparison with previous investigations verifies the dependence of the curves shown in Figs. 12 and 16 on Mach number.

Ref. 5 contains a theoretical development, for selected probe geometries, which predicts a viscous correction for impact pressures in supersonic, continuum, viscous flow. This development assumes a normal shock wave and includes the viscous effects in the subsonic flow field by means of a boundary layer analysis. This theory predicts that the impact pressure sensed in a viscous fluid is always larger than the ideal non-viscous impact pressure.

The results obtained in this investigation are in variance with this theory. As pointed out previously, other investigations at lower Mach numbers, with source-shaped probes, have shown measured impact pressures higher than the ideal. It is apparent that for certain Reynolds number and Mach number ranges, the theory given in Ref. 5 is invalid for impact-pressure probes of the types used in this investigation.

A theoretical analysis of impact pressure by Staros (Ref. 8),

based on the entropy rise and the related dissipation behind a detached normal shock, predicts that measured impact pressures in a viscous supersonic flow are less than the ideal non-viscous impact pressures. For the range of Mach numbers and Reynolds numbers encountered in the present investigation, it appears that this theoretical analysis is qualitatively correct.

B. Total-Temperature Probe Calibration

1. Initial Calibration for Comparison of Probes A and B

Total-temperature Probes A and B were initially calibrated at a constant total temperature of 225°F. The choice of total temperature was based on two considerations: the temperature chosen was sufficiently high to prevent condensation of the constituents of the air in the wind tunnel test section and was sufficiently low for it to be maintained over the operational range of reservoir pressures. The Mach number was not constant over the range of test conditions but tended to vary slightly with decreasing reservoir pressure and increasing total temperature. Unavoidable variation of the boundary layer thickness in the nozzle produced this variation of Mach number.

Test conditions for the initial calibrations are summarized as follows:

$$p_o(\text{psia}) = 14.7 \text{ to } 94.7$$

$$\text{Re/inch} = 30{,}800 \text{ to } 213{,}000$$

$$M = 5.5 \text{ to } 5.8$$

The results of the initial calibration are presented in Fig. 17. The

variation of the temperature recovery factor is plotted as a function of the Reynolds number based on free stream conditions and the probe entrance outside diameter. For calculation of the temperature recovery factor, adiabatic flow from the temperature probe located just ahead of the nozzle throat to the total-temperature probe in the test section was assumed.

The temperature recovery factor for Probe B was considerably lower than that for Probe A. However, the general shape of the two calibration curves is similar. The relatively poor performance of Probe B can be partially attributed to its smaller entrance diameter. Evidently, the smaller diameter shield is less effective than the large diameter shield, and hence allows more conduction and radiation losses from the stagnation streamline. The shield on Probe B is also somewhat longer than that on Probe A. The increased shield length is also conducive to more heat loss. It would be expected that, since the length to diameter ratios of the thermocouple wires for the two probes are essentially equal, the conduction loss through the thermocouple wires would be approximately the same.

No additional calibrations were made for Probe B at other reservoir pressures; instead, Probe A was chosen for more extensive calibration analysis.

2. Extended Calibration of Probe A

Probe A was calibrated for the operating range of reservoir pressures at three total temperatures. The range of total temperatures used was restricted due to the considerations previously mentioned.

Three series of data were recorded for essentially the same range of Reynolds numbers and Mach numbers at constant total temperatures of 220°F, 225°F, and 260°F, respectively. Test conditions for these calibration runs are summarized as follows:

$$P_o = 14.7 \text{ to } 94.7 \text{ psi}$$
$$Re = 30{,}800 \text{ to } 213{,}000$$
$$M = 5.5 \text{ to } 5.8$$

The results of the calibration of Probe A are presented in Figs. 18-20. The temperature recovery factor is presented as a function of three different parameters, Re, Nu, and Nu^*, in an attempt to show the effect of the total-temperature change on the calibration curves. The only curve which shows a distinguishable effect due to total temperature change is the one based on the parameter Nu^* shown in Fig. 20. Thus, it is noticed that the temperature recovery factor is apparently highest for a given value of Nu^* at the lowest total temperature. It should be noted here that the calibration curves obtained in this investigation are quantitatively valid only for the particular probes used in the tests.

3. Suitability of Parameters for Presenting Temperature Recovery Factor Calibrations

The ideal parameter to use in plotting a calibration curve is one which is based on properties of the free stream and which yields a single curve valid over a considerable range of flow conditions. The Reynolds number based on properties of the free stream provides a convenient parameter, and the results of this investigation show that use of this parameter produces a single curve for this range of test con-

ditions. The Nusselt number based on flow conditions inside the probe and on the thermocouple wire diameter also produces a single curve over the range of test conditions. It is difficult, however, to justify theoretically the significance of either of these parameters, and it could not be expected that use of either Reynolds number or Nusselt number would produce a single curve for large variations of Mach number or total temperature. It should be noted that the Nusselt number of the flow within a given probe geometry can be related to the properties of the free stream. The only properties required to obtain the Nusselt number are the total temperature and the impact pressure.

An attempt was made to determine theoretically a significant parameter based on flow conditions inside the temperature probe. This theoretical analysis is presented in Appendix A and is based on considerations of a simplified theory of heat transfer. For the purposes of the problem, it was assumed that heat losses other than conduction through the thermocouple wires are negligible. This analysis indicates the significance of the parameter $Nu\ k_g/k_w$, which is proportional to Nu^* (defined by Eq. 18), this factor of proportionality being constant for a given probe geometry. The theoretical results shown in Appendix A indicate that the temperature-recovery factor, when plotted versus Nu^*, should be invariant with respect to total temperature and the free stream Mach number.

As previously noted, use of the parameter Nu^* does not yield a single calibration curve. It appears, therefore, that the assumptions made in the theoretical analysis are perhaps over simplified, and consequently do not provide a sufficiently accurate analysis for the temperature probe used in this investigation. It is believed, however,

that for variable free stream Mach numbers this parameter would prove superior to those based on free stream conditions.

4. Comparison with a Previous Experimental Investigation

By using the parameter Nu k_g/k_w, which is as mentioned previously proportional to what is defined in this study as Nu^*, E. Winkler, Ref. 11, has obtained a single calibration curve valid for a considerable range of total temperatures, Reynolds numbers, and hypersonic Mach numbers. For the probe calibrated in Ref. 11, it was estimated that 95 per cent of the total heat losses was due to conduction through the thermocouple wires. The results obtained in this investigation are somewhat different from those of Ref. 11. This variance might be partially attributed to the shielding employed on Probe A not being as effective as the shielding used for the probes calibrated in Ref. 11. Less effective shielding would make more inaccurate the assumptions used in Appendix A, which theoretically establish Nu^* as being a significant parameter. It would then be expected that a probe which had relatively inadequate shielding with consequent increased losses from the stagnation streamline would not, for a given value of Nu^*, have a temperature recovery factor constant with respect to total temperature.

Experimental data given in Ref. 11 show a dependence on total temperature of a plot of temperature recovery factor versus Reynolds number. In Ref. 11, the total-temperature changes were quite large; therefore, the dependence on total temperature was easily detected. As previously pointed out, for the limited total-temperature range available in this investigation and for the curve of temperature recovery factor

versus Reynolds number shown in Fig. 18, any effect due to change in total temperature was not apparent within the normal scatter of the experimental data. It is expected that if the range of temperatures could have been extended, the effect of the change of total temperature would have become apparent.

V. CONCLUSIONS AND RECOMMENDATIONS

With regard to the impact-pressure phase of this investigation at a nominal Mach number of 5.6, the results indicate the detection of viscous effects on the readings of impact-pressure probes at Reynolds numbers as high as 6000. While the effects are negligible at this Reynolds number, they continue to increase with decreasing Reynolds numbers, and at a Reynolds number of 425 the measured impact pressure is approximately 2.5 per cent lower than that predicted by the Rayleigh equation. A comparison of the two probe geometries tested indicates that the flattened-end probes are more susceptible to these viscous effects at the lower Reynolds numbers than are the circular end probes. It appears definitely that this investigation should be extended to higher Mach numbers and lower Reynolds numbers, since both of these variations tend to increase the viscous effects on impact-pressure determination.

The total-temperature phase of this investigation involved the calibration of a particular temperature probe and an analysis of various parameters suitable for presenting this calibration. For the nominal Mach number of 5.6 and total temperatures from 200°F to 260°F, a single calibration curve of temperature recovery factor was obtained with the use of the Reynolds number of the free stream based on the probe entrance outside diameter or the Nusselt number of the flow inside the probe based on the thermocouple wire diameter. The data show that the temperature recovery factor of the total-temperature probe decreases with decreasing Reynolds numbers. Here again it seems desirable to extend the investigation to higher Mach numbers, lower Reynolds numbers, and a wider range of total temperatures.

REFERENCES

1. Sherman, F. S.: "New Experiments on Impact-Pressure Interpretation in Supersonic and Subsonic Rarefied Air Streams", NACA TN 2995, 1953.

2. Kane, E. D. and Maslach, G. J.: "Impact-Pressure Interpretation in a Rarefied Gas at Supersonic Speeds", NACA TN 2210, 1950.

3. Kane, E. D. and Schaaf, S. A.: "Viscous Effects on Impact Probes in a Subsonic Rarefied Gas Flow", Report No. HE-150-82, Univ. of California, March 9, 1951.

4. Chambre, P. L. and Smith, H. R.: "The Impact Tube in a Viscous Compressible Gas", Report No. HE-150-63, Univ. of California, August 29, 1948.

5. Chambre, P. L.: "The Theory of the Impact Tube in a Viscous Compressible Gas", Report No. HE-150-50, Univ. of California, November 1, 1948.

6. Chambre, P. L. and Schaaf, S. A.: "The Theory of the Impact Tube at Low Pressures", Jour. Aero. Sci., Vol. 15, No. 12, December 1948, pp. 735-737.

7. Murphy, S.: "Evidences of an Inherent Error in Measurement of Total-Head Pressure at Supersonic Speeds", Aero. Eng. Review, Vol. 12, No. 11, November 1953, pp. 47-51.

8. Staros, B.: "Investigation of Effect of Energy Dissipation Behind a Detached Shock Wave on Total-Head Measurements", Ae.E. Thesis, California Institute of Technology, 1950.

9. Liepmann, H. W. and Puckett, A. E.: "Introduction to Aerodynamics of a Compressible Fluid", John Wiley and Sons, Inc., New York, 1947.

10. Tsien, H. S.: "Superaerodynamics, Mechanics of Rarefied Gases", Jour. Aero. Sci., Vol. 13, No. 12, December 1946, pp. 653-664.

11. Winkler, E. M.: "Design and Calibration of Stagnation Temperature Probes for Use at High Supersonic Speeds and Elevated Temperatures", Jour. of App. Physics, Vol. 25, No. 2, 231-232, February 1954.

12. Goldstein, D. L. and Scherrer, R.: "Design and Calibration of a Total-Temperature Probe for Use at Supersonic Speeds", NACA TN 1885, 1949.

13. Hottel, H. C. and Kalitinsky, A.: "Temperature Measurements in High-Velocity Air Streams", Jour. of App. Mech., March 1945, pp. A25-A32.

14. Hypersonic Wind Tunnel Staff: "Charts and Tables for Analysis of Hypersonic Flow", California Institute of Technology, Guggenheim Aeronautical Laboratory, Hypersonic Wind Tunnel Memorandum No. 4, May 1951.

15. Eimer, M.: "Direct Measurement of Laminar Skin Friction at Hypersonic Speeds", Ph.D. Thesis, California Institute of Technology, 1953.

16. Morey, F. C.: "NBS-NACA Tables of Thermal Properties of Gases", Table 2.39, December 1950.

17. Chapman, S.: "On the Law of Distribution of Molecular Velocities, and on the Theory of Viscosity and Thermal Conduction, in a Non-Uniform Simple Monatomic Gas", Phil. Trans. Roy. Soc., Vol. 216(A), pp. 279348, 1915.

18. Scadron, M. D. and Warshawsky, I.: "Experimental Determination of Time Constants and Nusselt Numbers for Bare-Wire Thermocouples in High-Velocity Air Streams and Analytical Approximation of Conduction and Radiation Errors", NACA TN 2599, 1952.

APPENDIX A

TEMPERATURE ERROR AT A THERMOCOUPLE JUNCTION DUE TO CONDUCTION IN THE THERMOCOUPLE WIRES

If it were possible to bring a fluid stream to rest adiabatically at a thermocouple junction, the kinetic energy of the stream would be completely recovered, and the fluid temperature at the junction would be the total temperature, T_o. With an actual temperature probe, it is impossible to achieve absolute adiabatic deceleration of the flow to stagnation. As the temperature of a fluid element in the stagnation streamline increases above the static temperature of the free stream, there is a loss of heat from the sample due to conduction of heat through the gas in addition to radiation and convective heat transfer to the probe shield.

However, according to Ref. 18, the heat loss due to non-adiabatic flow along the stagnation streamline and the heat loss from the thermocouple junction by radiation are considered to be relatively small compared to the heat loss from the junction by conduction through the thermocouple wires. Consequently, for this analysis, only the heat loss due to conduction through the thermocouple wire is considered. To evaluate this effect it is assumed that there exists a uniform fluid temperature, T_o, along the bare thermocouple wire and that there is a negative temperature gradient from the thermocouple junction to the base of the wire. It is also assumed that the temperature of the wire is constant at any cross section.

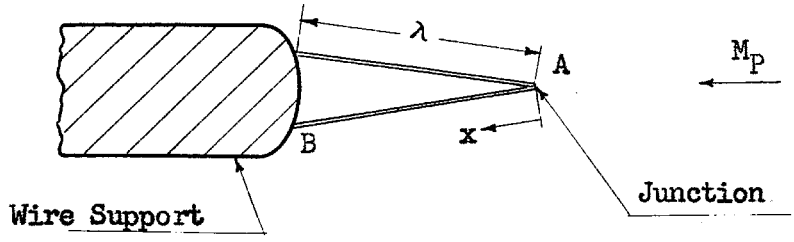

Referring to the above sketch, the temperature of the wire at A, T_A, must be greater than the temperature at B, T_B, in order for heat to flow from A to B. Also, $(dT/dx)_A = 0$ by symmetry, and the velocity inside the probe, u_p, is assumed small so that $(u_p^2)/(2g\ J\ C_p\ T_o) << 1$.

Considering an element of wire of length dx, the heat flux, Q, through the wire at a given cross section is

$$Q = \left(- \frac{dT_w}{dx} \right) k_w \frac{\pi d_w^2}{4} \qquad (A\text{-}1)$$

where k_w is the coefficient of thermal conductivity of the wire. Then at a point a distance, dx, from the given cross section the heat flux is given by

$$Q + dQ = - \left(\frac{dT_w}{dx} \right) + \left(\frac{d^2 T_w}{dx^2} \right) dx\ k_w \frac{\pi d_w^2}{4} \qquad (A\text{-}2)$$

and the increment of heat flux in the element of wire of length dx is

$$dQ = - \frac{d^2 T_w}{dx^2}\ dx\ k_w \frac{\pi d_w^2}{4} \qquad (A\text{-}3)$$

Now consider the heat flux from the fluid to the wire through the surface of the wire element. This may be written

$$dQ = (T_o - T_w)\ h\ \pi d_w\ dx \qquad (A\text{-}4)$$

where T_o is the stagnation temperature of the fluid, $T_w(x)$ is the local

temperature of the wire, and h is the convective heat transfer coefficient which includes the combined effect of conduction through the film and convection in the fluid. This coefficient is assumed to be constant over the length of the wire.

Now, for equilibrium conditions to exist in the wire, the heat flux through the surface must equal the change of heat flux along the thermocouple wire. Thus, the resulting differential equation is

$$\frac{d^2T_w}{dx^2} - \frac{4h}{k_w d_w}(T_w - T_o) = 0 \qquad \text{(A-5)}$$

It is convenient now to introduce the Nusselt number, in the form

$$Nu = h\, d_w/k_g \qquad \text{(A-6)}$$

where k_g is the coefficient of thermal conductivity of the fluid. Then, denoting the cross sectional area of the wire by A, Eq. A-5) becomes

$$\frac{d^2 T_w}{dx^2} - Nu\, \frac{k_g}{k_w}\, \frac{1}{\pi A}\, (T_w - T_o) = 0 \qquad \text{(A-7)}$$

The general solution of this differential equation is

$$T_w - T_o = c_1 e^{-\beta x} + c_2 e^{\beta x} \qquad \text{(A-8)}$$

where

$$\beta^2 = Nu\, (k_g/k_w)(1/\pi A) \qquad \text{(A-9)}$$

Now, if the boundary conditions are applied

$$c_1 = c_2\, \frac{T_B - T_o}{e^{-\beta\lambda} + e^{\beta\lambda}} \qquad \text{(A-10)}$$

and

$$T_o - T_w = \frac{(T_o - T_B)\cosh \beta x}{\cosh \beta\lambda} \qquad \text{(A-11)}$$

where λ is the length of wire between points A and B in the previous sketch. At the thermocouple junction, $x = 0$, $T_w = T_o'$, and Eq. (A-11) becomes

$$T_o - T_o' = \frac{T_o - T_B}{\cosh \beta\lambda} \tag{A-12}$$

The energy equation for adiabatic, frictionless, steady flow of a perfect gas may be written

$$T_o - T = \frac{u^2}{2g\ J\ c_p} \tag{A-13}$$

and by the use of the definition of the temperature recovery factor, r, at the thermocouple junction, this equation becomes

$$T_o' - T = r\ \frac{u^2}{2g\ J\ c_p} \tag{A-14}$$

or

$$T_B - T = r_B\ \frac{u^2}{2g\ J\ c_p} \tag{A-15}$$

where r_B is the temperature recovery factor of the thermocouple base (Point B).

Combining Eqs. (A-12), (A-14), and (A-15) yields the following expression for recovery factor

$$r = 1 - \frac{(1 - r_B)}{\cosh \beta\lambda} \tag{A-16}$$

It is clear that for a given probe geometry, $r = r(r_B, \beta)$, where β is defined in Eq. (A-9). Thus, the significance of the parameter Nu (k_g/k_w) can be easily seen.

APPENDIX B

ACCURACY ANALYSIS OF EXPERIMENTAL DATA

The magnitude of the random errors encountered were estimated by considering the reproducibility of the observations, the sensitivity of the scale, and the associated reading error. For the experimentally measured quantities, these estimated errors are as follows:

Measurement	Estimated Maximum Error
Static pressure - p	$\pm$0.2 mm. of silicone
Impact pressure - p_o"	$\pm$0.5 mm. of silicone
Reservoir pressure - p_o	less than 0.5%
Reservoir temperature - T_o	$\pm 2^{\circ}F$
Thermocouple voltage	$\pm$0.01 micro volt
Impact tube dimension d,h	$\pm$.0005 inch

The ideal impact pressure was obtained by an extrapolation procedure as explained in Section III. The estimated maximum probable error in the extrapolated value of impact pressure is $\pm$0.5 mm. of silicone. This estimated value was determined as a result of a graphical study of the extrapolation curves.

The accuracy of the computed values, based on both estimated errors in the individual measurements and the errors from the use of graphs, tables, etc., is as follows:

Quantity	Maximum Error
Ratio of impact pressures - p_o''/p_o'	$\pm$ 0.12%
Mach Number - M	$\pm$ 1%
Free Stream Temperature - T	$\pm$ 2%
Reynolds Number - Re	$\pm$ 5.5%
Temperature Recovery Factor - r	$\pm$ .06%

LIST OF FIGURES

		PAGE
1.	GALCIT 5 x 5 Inch Hypersonic Wind Tunnel Controls and Instrumentation	41
2.	Schematic Diagram of GALCIT 5 x 5 Inch Hypersonic Wind Tunnel Installation	42
3.	Impact-Pressure Probe Rake	43
4.	Sketch of Impact-Pressure Probe Geometry, Types I and II	44
5.	Sketch of Stagnation-Temperature Probes A and B	45
6.	Temperature, Impact, and Static-Pressure Probe Support	46
7.	Schematic Diagram of Electrical Connection for the Thermo-couple-Potentiometer System	47
8.	Vertical Total-Head Survey in Leg No. 1	48
9.	Schlieren Picture of Air Flow about Probe Rake	49
10.	Sample Extrapolation Plots of Impact Pressure for Type II Probes	50
11.	Variation of Measured Impact Pressures with Reynolds Number for Type I Probes	51
12.	Variation of Measured Impact Pressures with Knudsen Number for Type I Probes	52
13.	Variation of Measured Impact Pressures with Reynolds Number Behind Normal Shock - Type I Probes	53
14.	Variation of Measured Impact Pressures with Knudsen Number Behind Normal Shock - Type I Probes	54
15.	Variation of Measured Impact Pressures with Reynolds Number for Type II Probes	55

16. Variation of Measured Impact Pressures with Knudsen Number for Type II Probes 56

17. Comparative Recovery Factors for Two Temperature Probes 57

18. Variation of Recovery Factor with Reynolds Number for Probe A 58

19. Variation of Recovery Factor with Nusselt Number for Probe A 59

20. Variation of Recovery Factor with Nu^* for Probe A 60

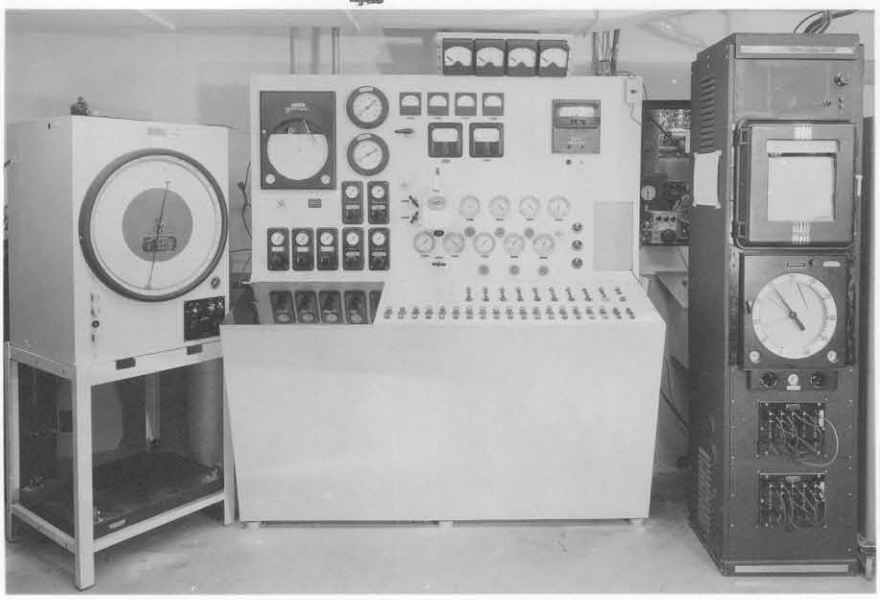

Compressor Plant Motor and Valve Controls
Reservoir Pressure and Temperature Regulators
Plant Pressure and Temperature Indicators

Fig. 1a

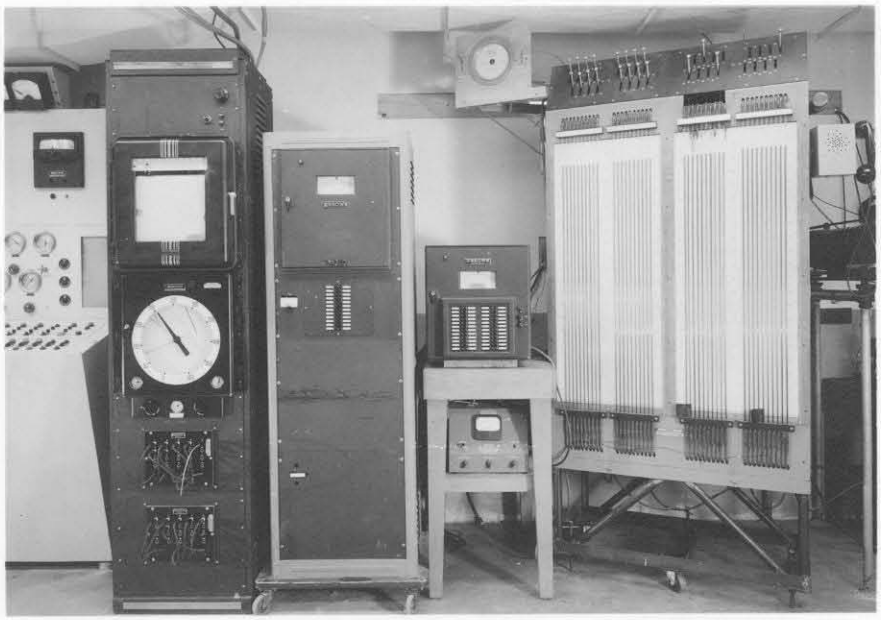

Test Section and Nozzle Block
Pressure and Temperature Instrumentation

Fig. 1b

GALCIT 5 x 5 IN. HYPERSONIC WIND TUNNEL
CONTROLS AND INSTRUMENTATION

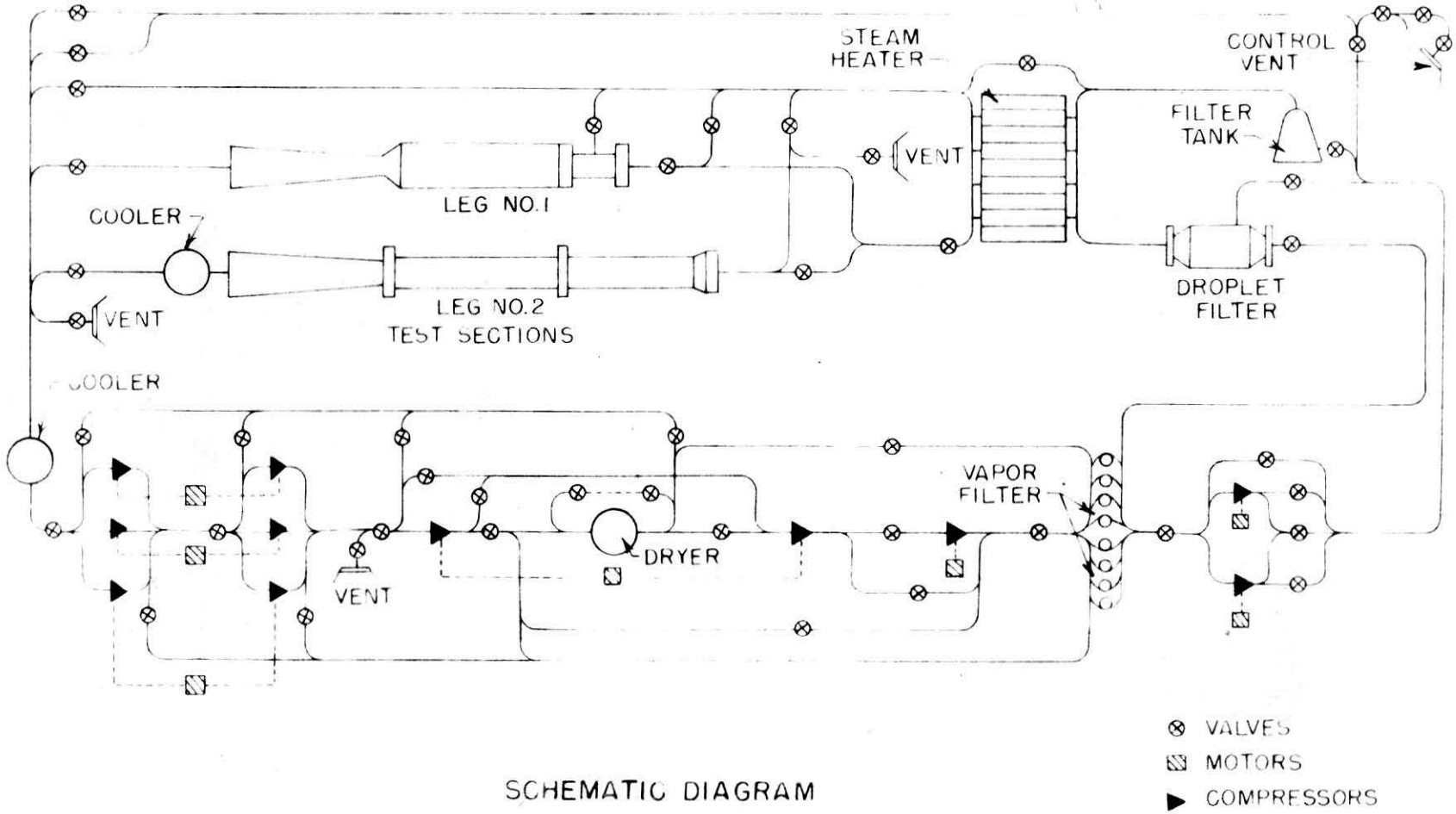

SCHEMATIC DIAGRAM

OF GALCIT 5x5in. HYPERSONIC WIND TUNNEL INSTALLATION

FIG.2

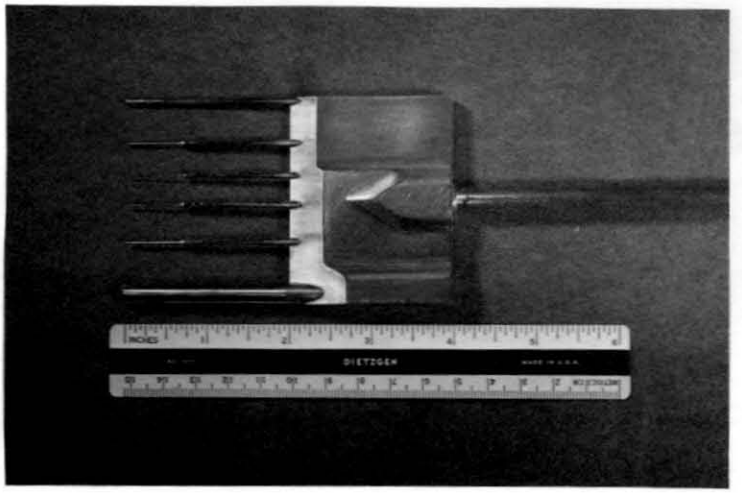

Type I Probes

Fig. 3a

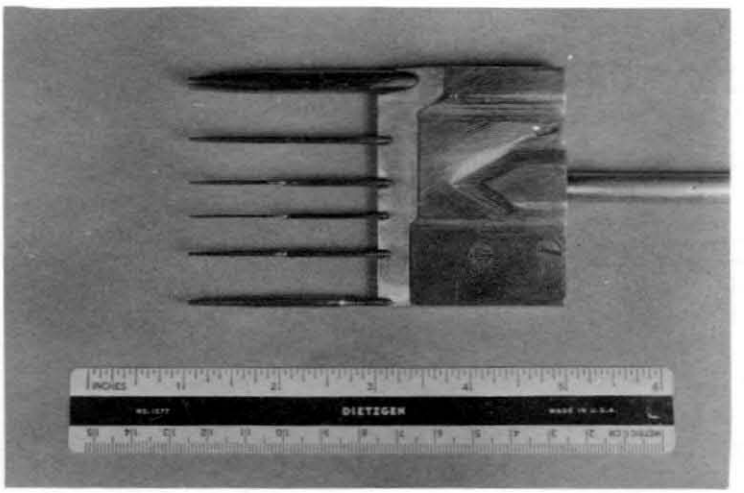

Type II Probes

Fig. 3b

IMPACT-PRESSURE PROBE RAKE

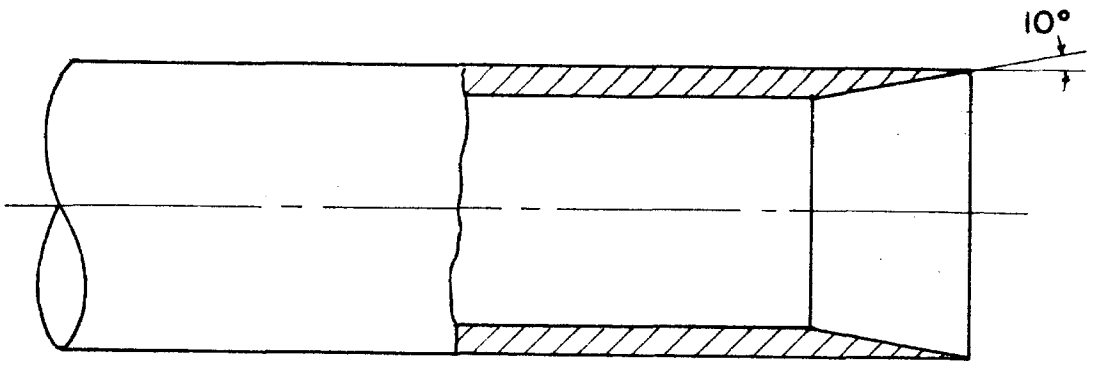

TYPE I - CIRCULAR-END TUBE

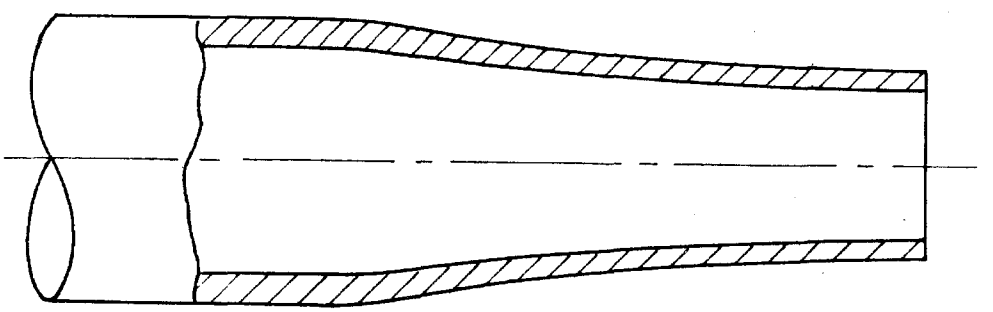

TYPE II - FLATTENED-END TUBE

SKETCH OF IMPACT-PRESSURE PROBE GEOMETRY

FIG. 4

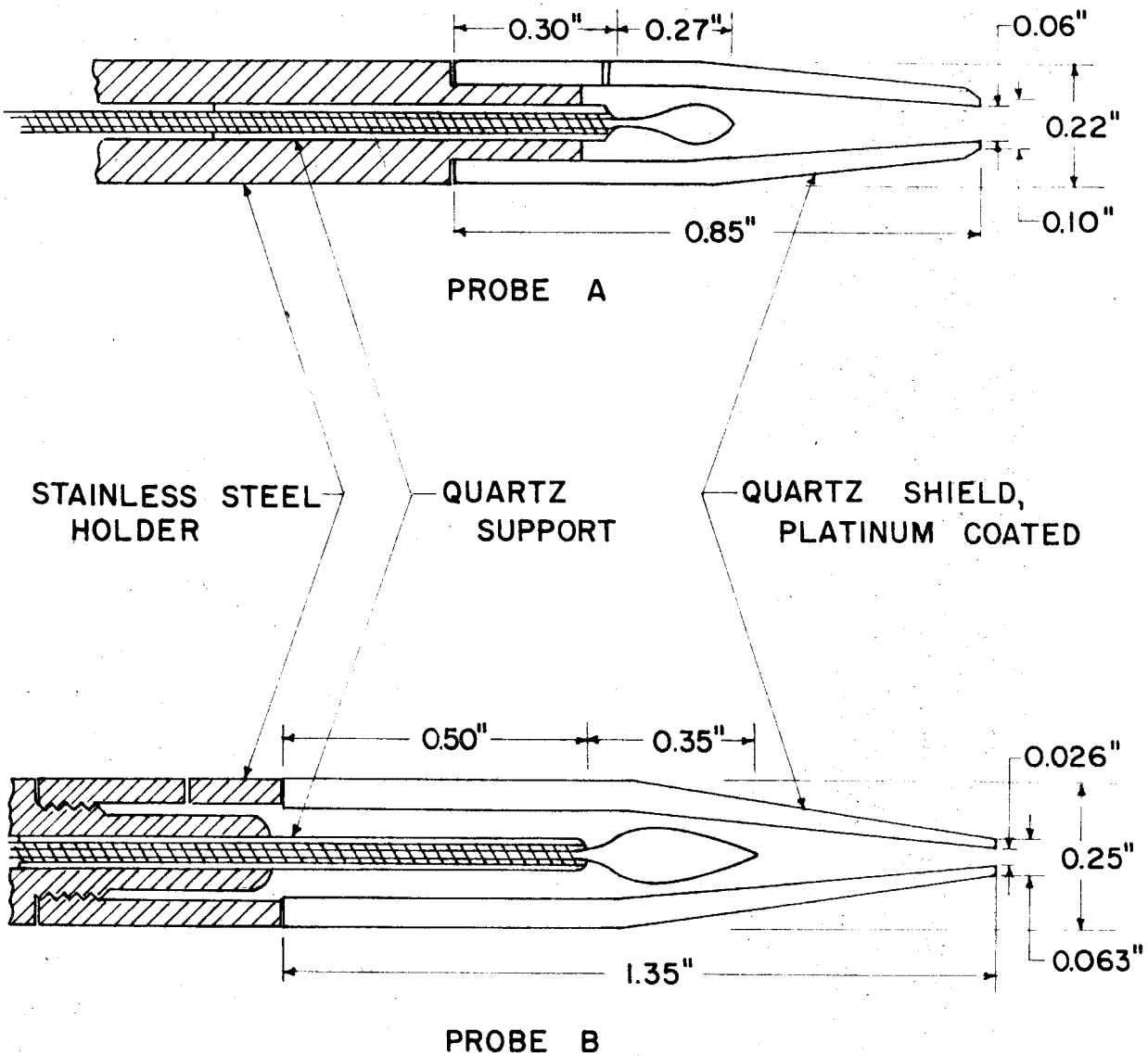

SKETCH OF STAGNATION-TEMPERATURE PROBES

FIG. 5

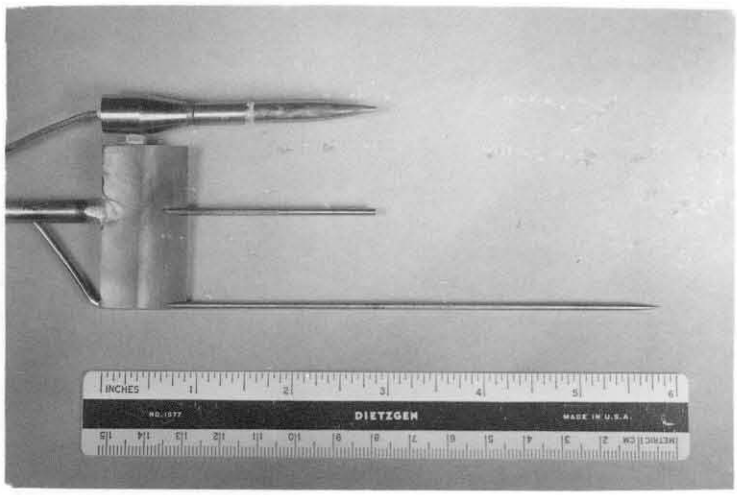

Fig. 6a

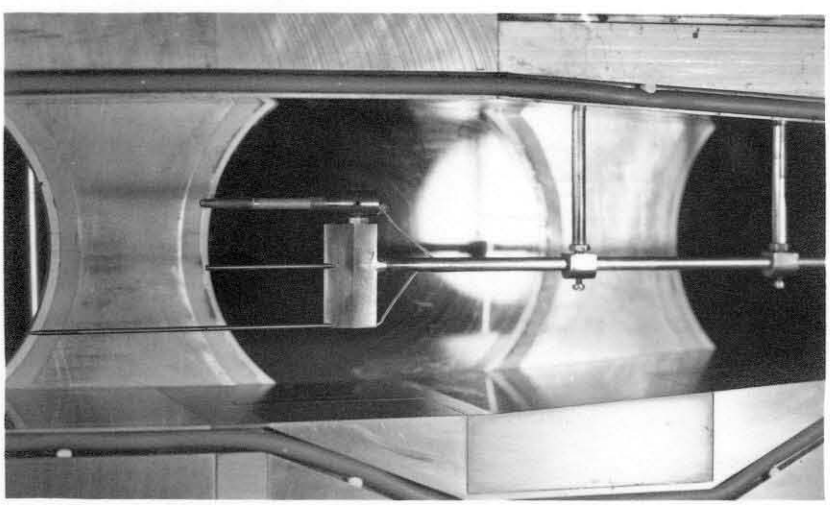

Fig. 6b

TEMPERATURE, IMPACT, AND STATIC-PRESSURE PROBE SUPPORT

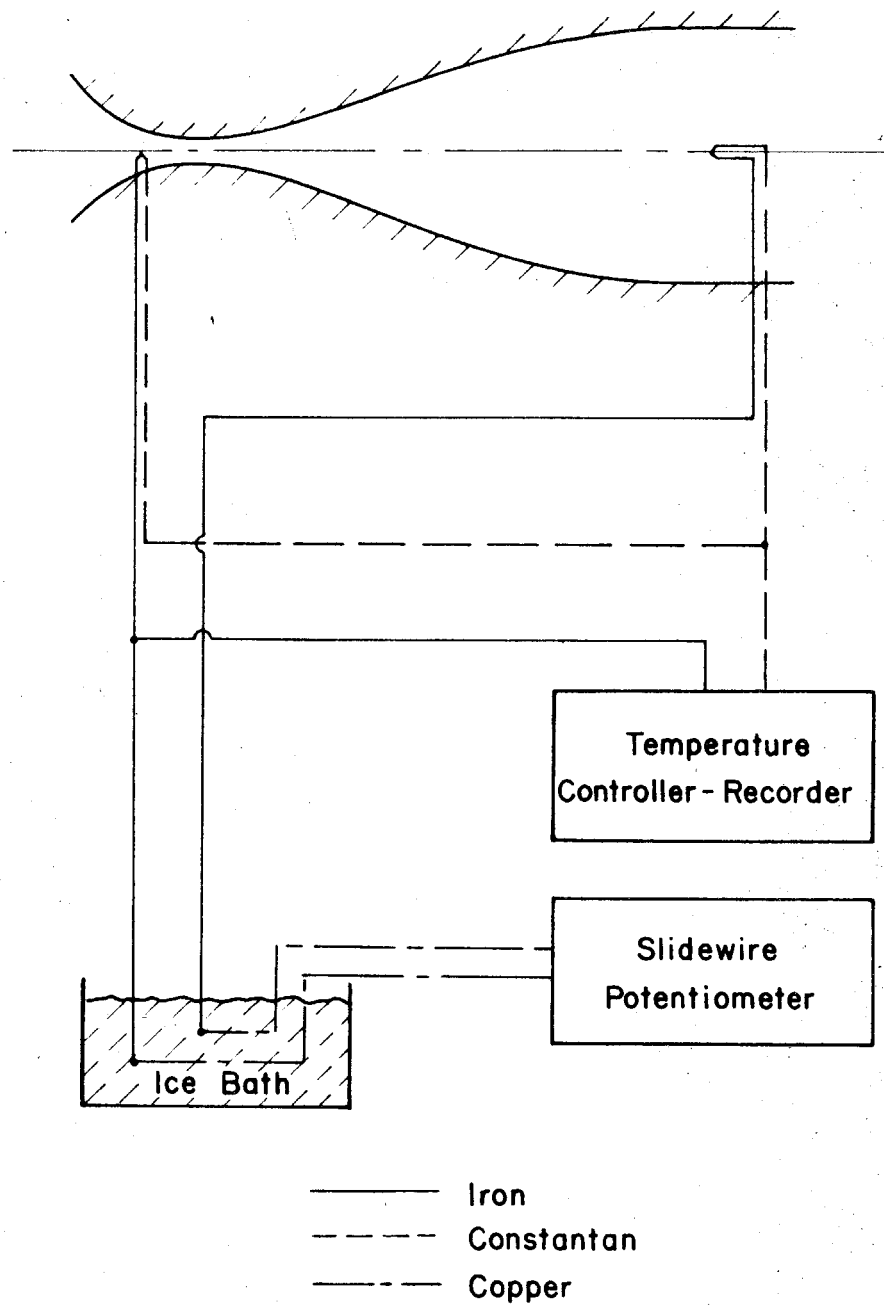

SCHEMATIC DIAGRAM OF ELECTRICAL CONNECTION FOR THERMOCOUPLE-POTENTIOMETER SYSTEM

FIG. 7

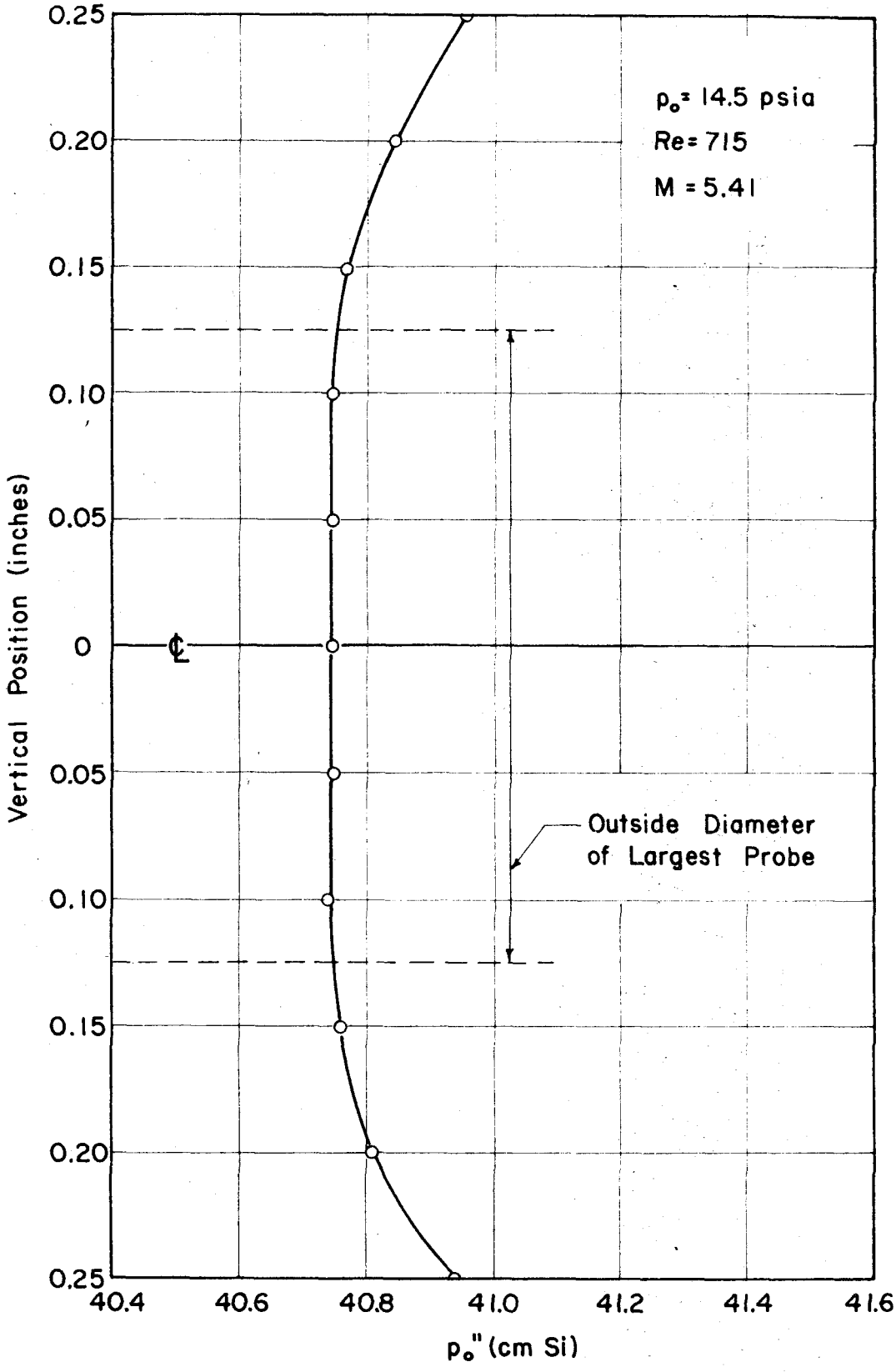

VERTICAL TOTAL-HEAD SURVEY IN LEG NO. 1

FIG. 8

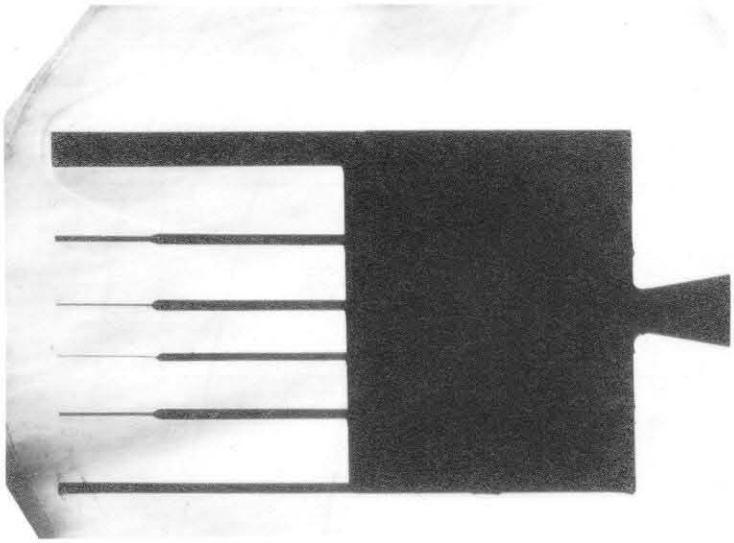

SCHLIEREN PICTURE OF AIR FLOW AROUND PROBE RAKE

Fig. 9

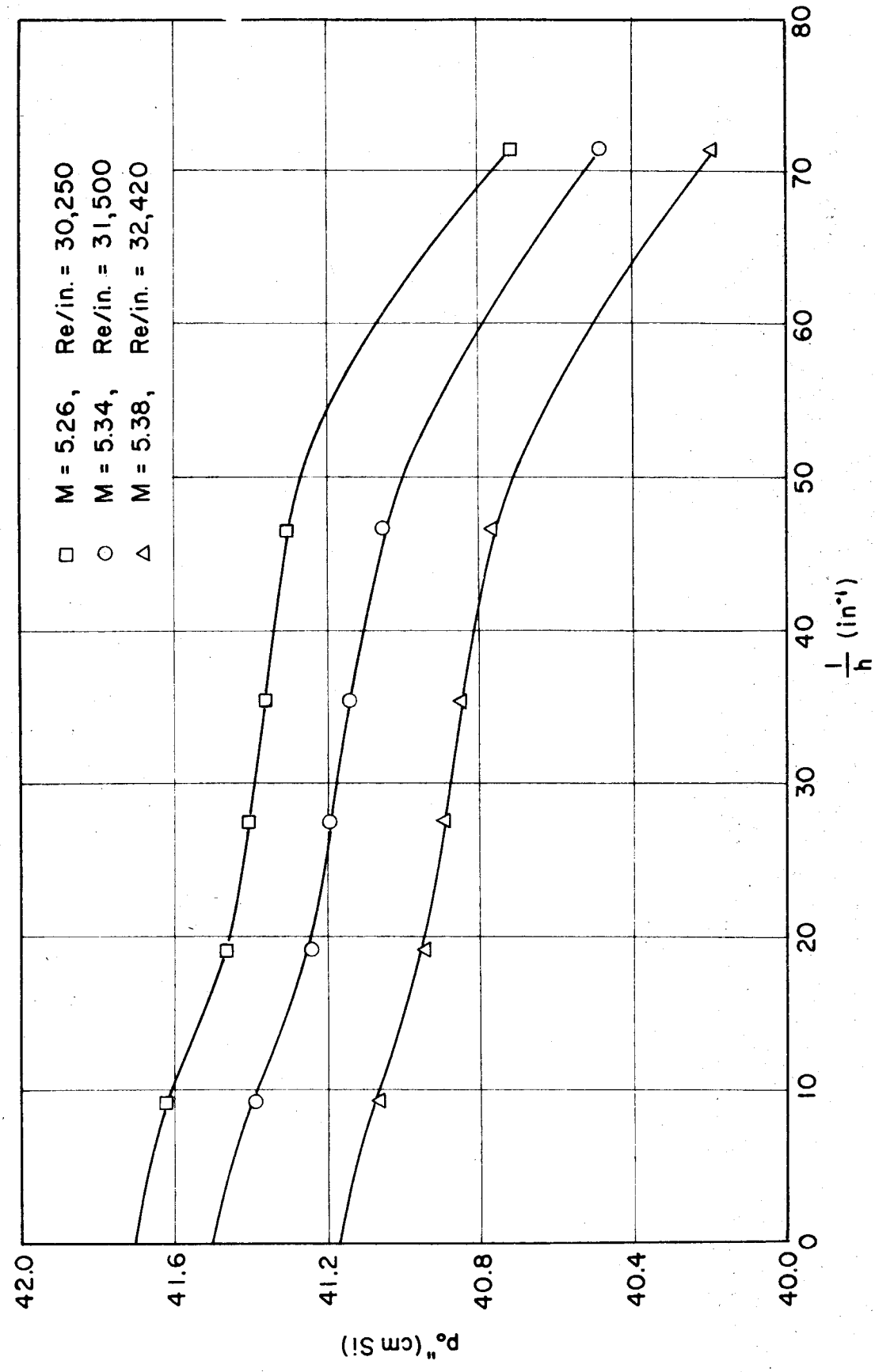

SAMPLE EXTRAPOLATION PLOTS OF IMPACT PRESSURE FOR TYPE II PROBES

FIG. 10

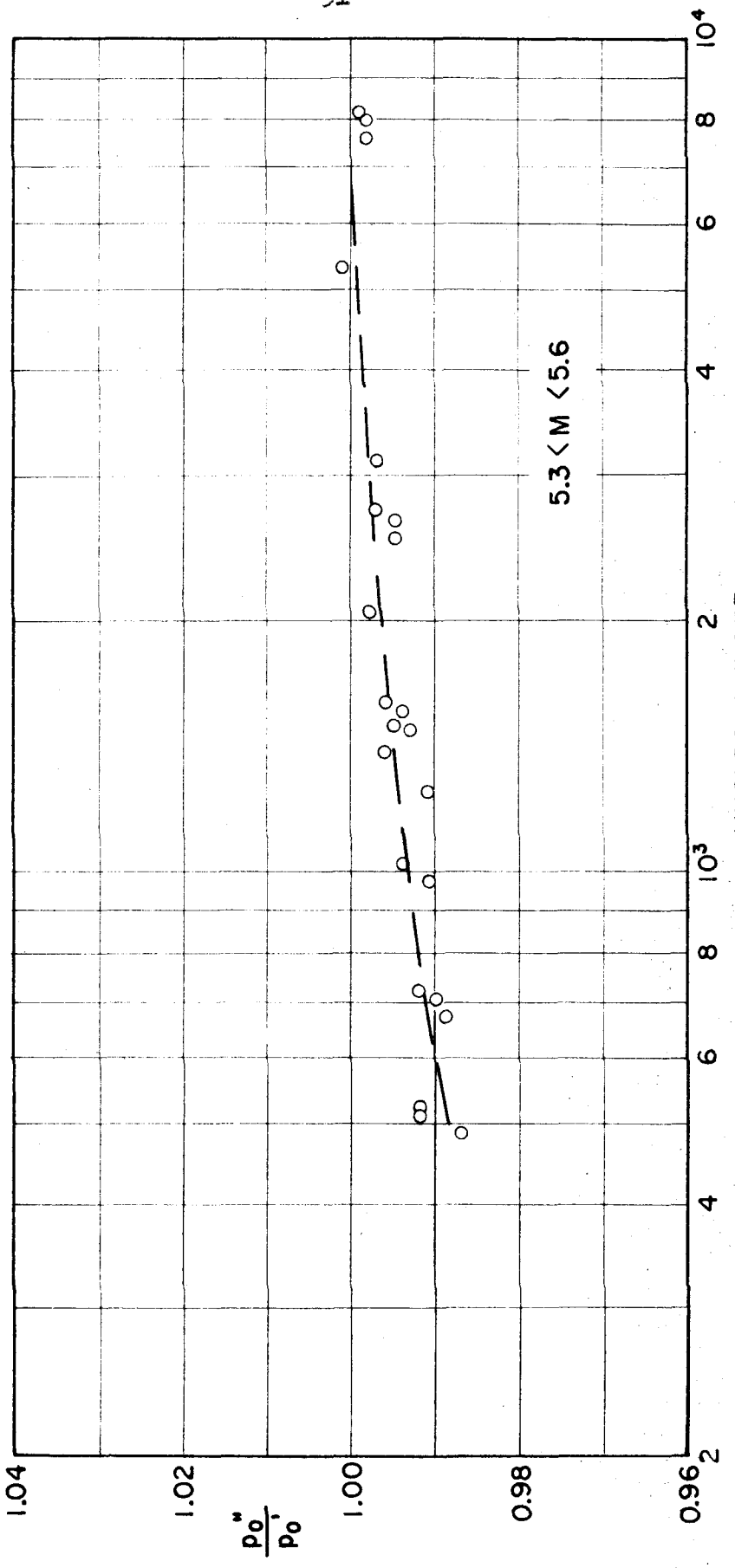

VARIATION OF MEASURED IMPACT PRESSURES WITH REYNOLDS NUMBER FOR TYPE I PROBES

FIG. 11

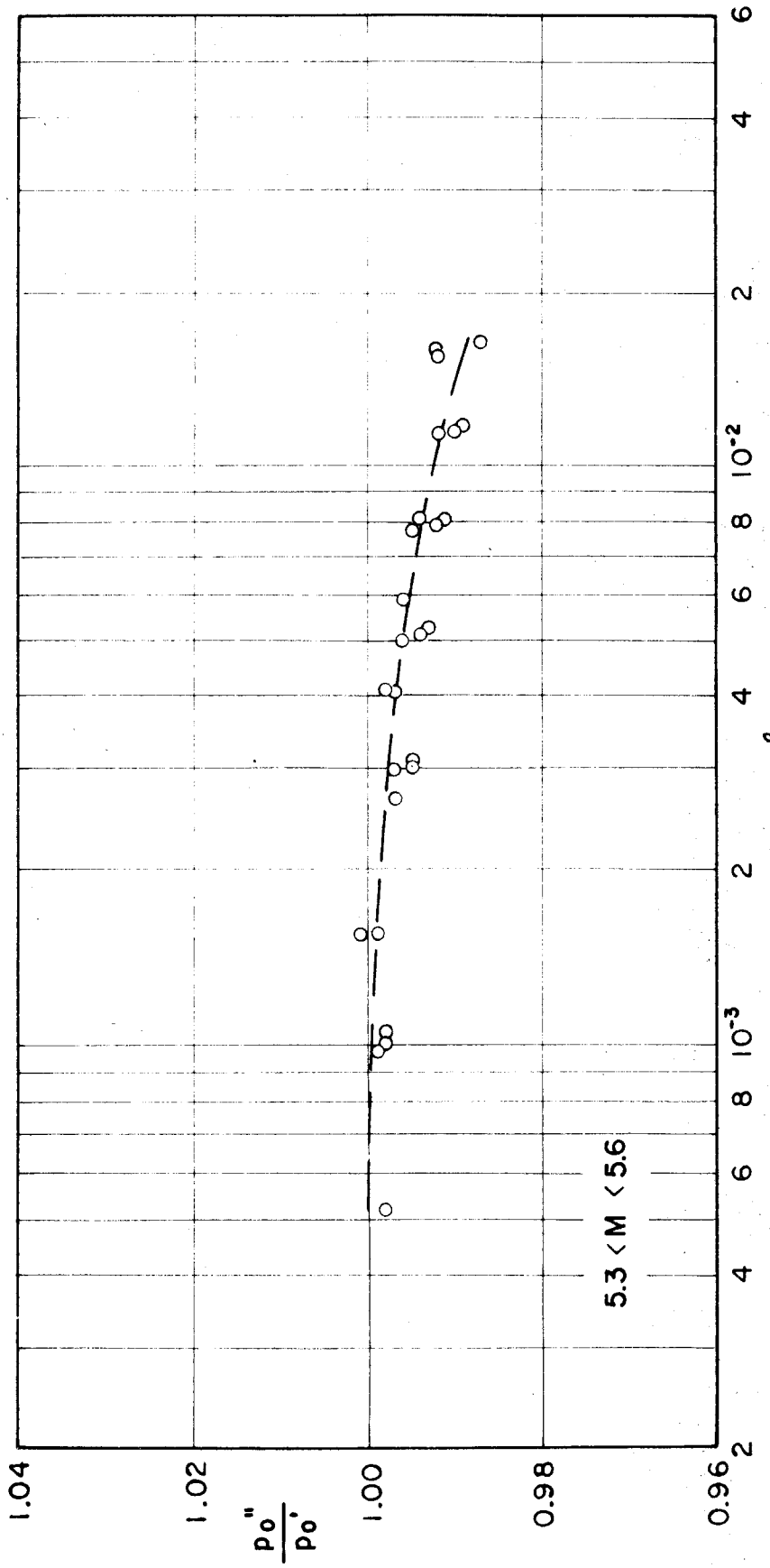

VARIATION OF MEASURED IMPACT PRESSURES WITH KNUDSEN NUMBER FOR TYPE I PROBES

FIG. 12

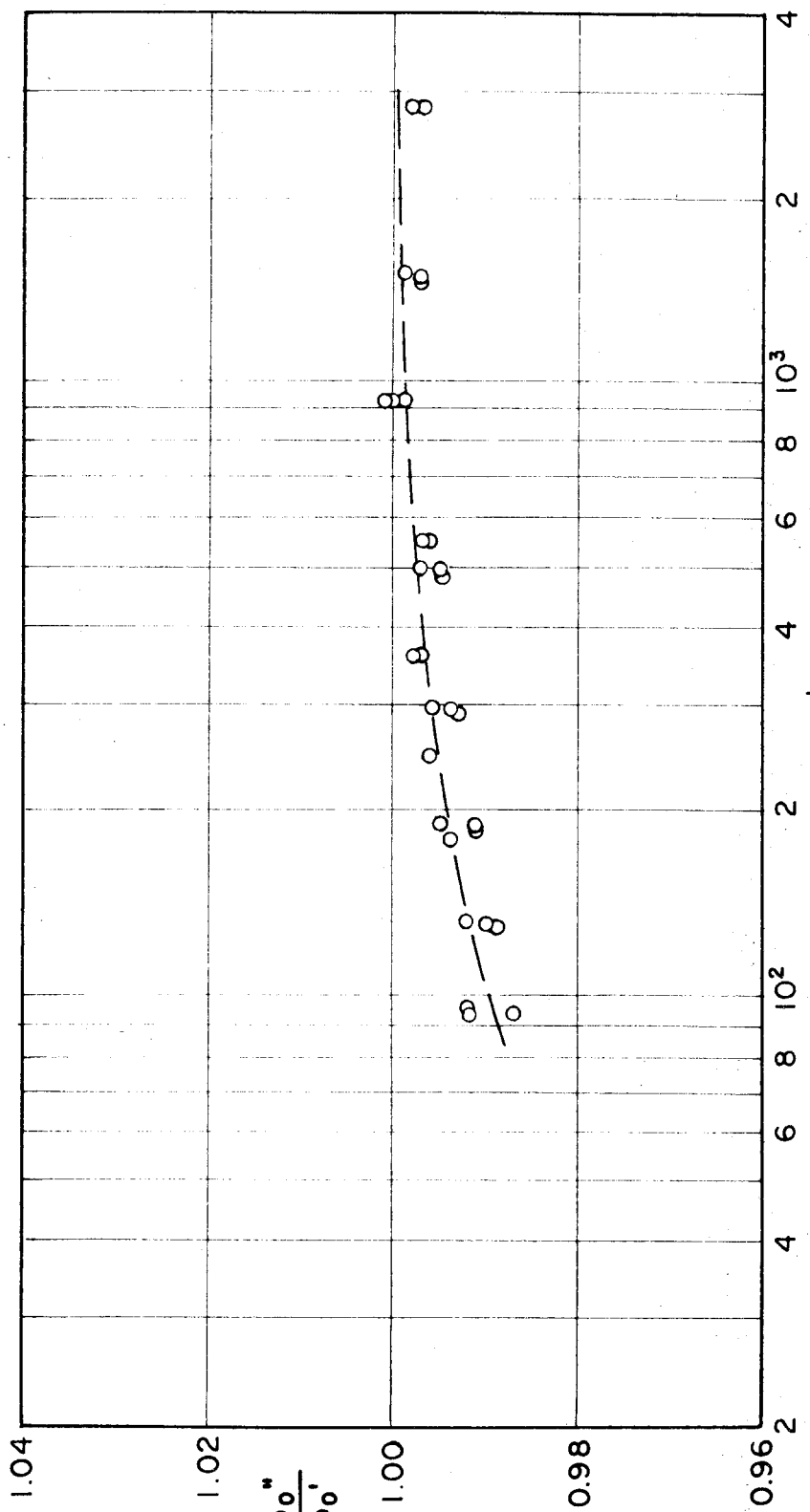

VARIATION OF MEASURED IMPACT PRESSURES WITH REYNOLDS NUMBER BEHIND NORMAL SHOCK FOR TYPE I PROBES

FIG. 13

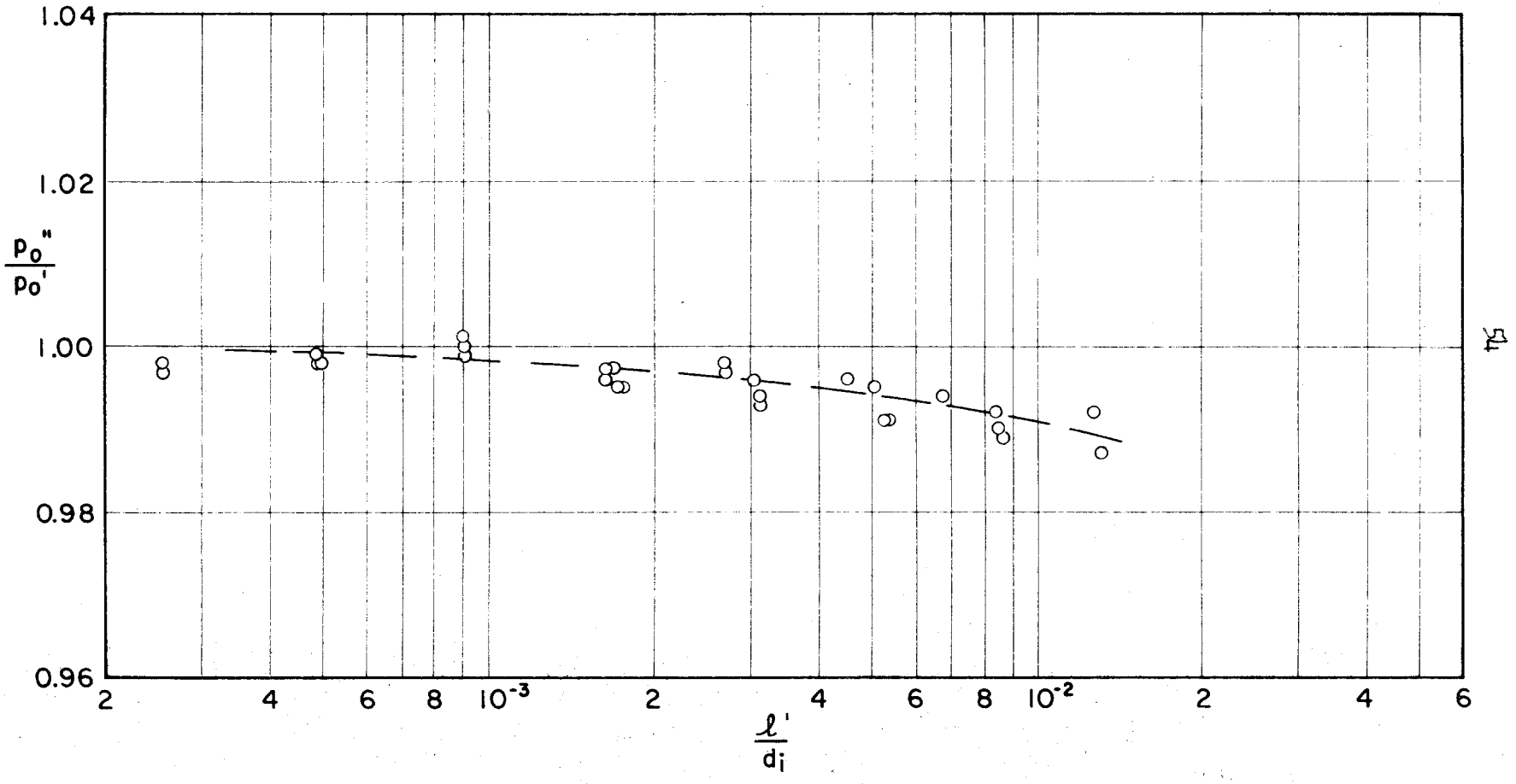

VARIATION OF MEASURED IMPACT PRESSURES WITH KNUDSEN NUMBER BEHIND NORMAL SHOCK FOR TYPE I PROBES

FIG. 14

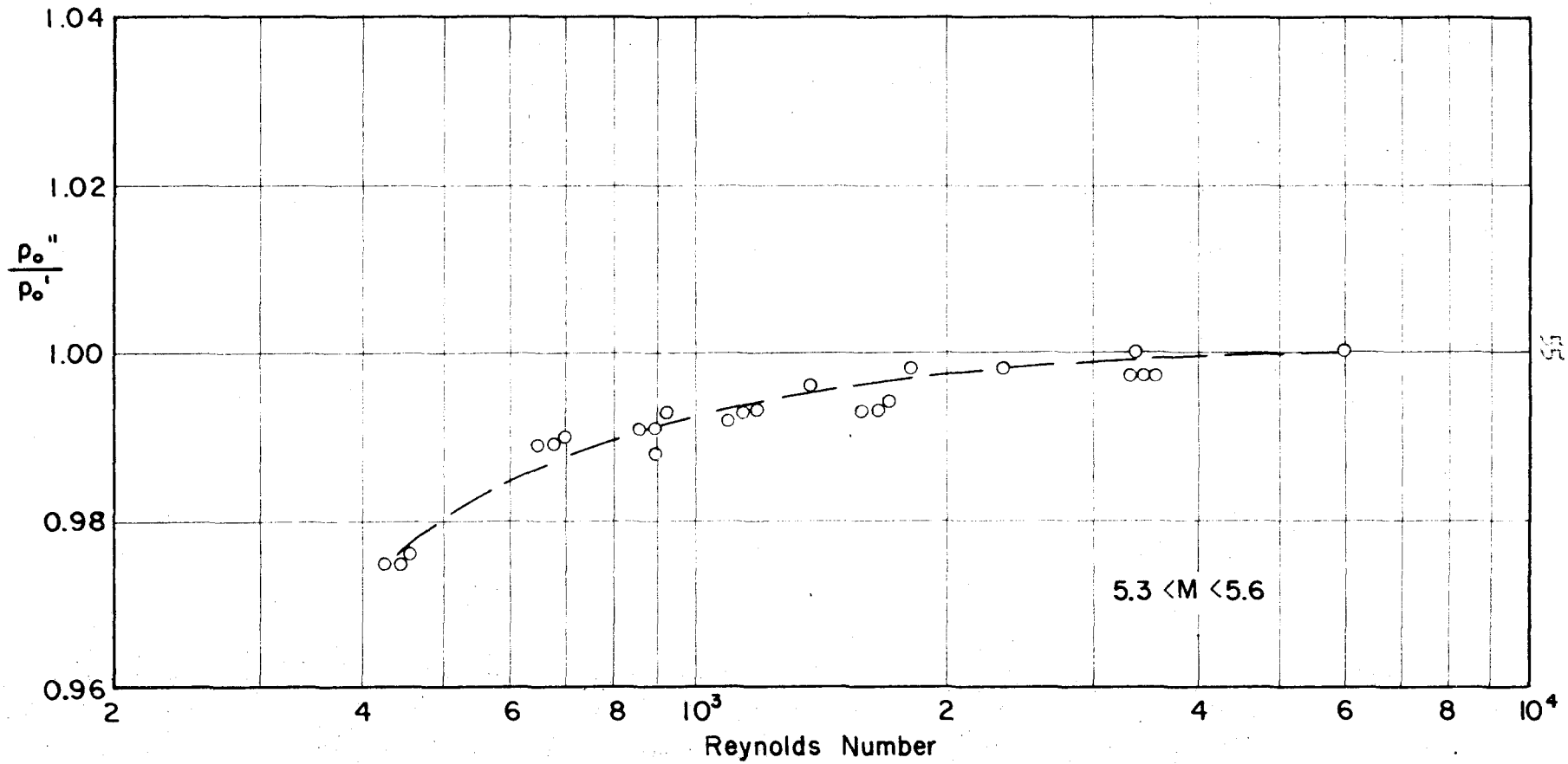

VARIATION OF MEASURED IMPACT PRESSURES WITH REYNOLDS NUMBER FOR TYPE II PROBES

FIG. 15

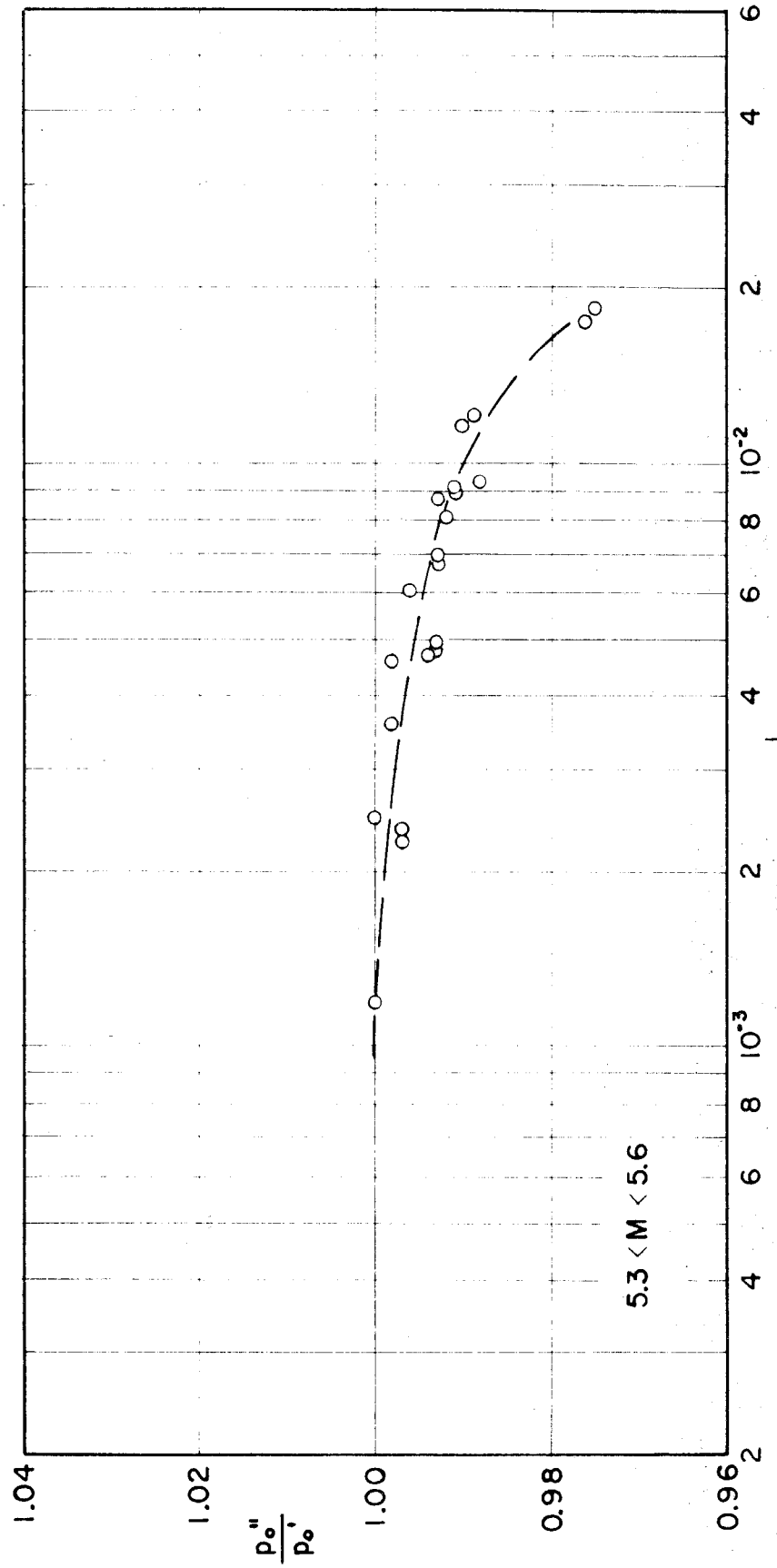

VARIATION OF MEASURED IMPACT PRESSURES WITH KNUDSEN NUMBER FOR TYPE II PROBES

FIG. 16

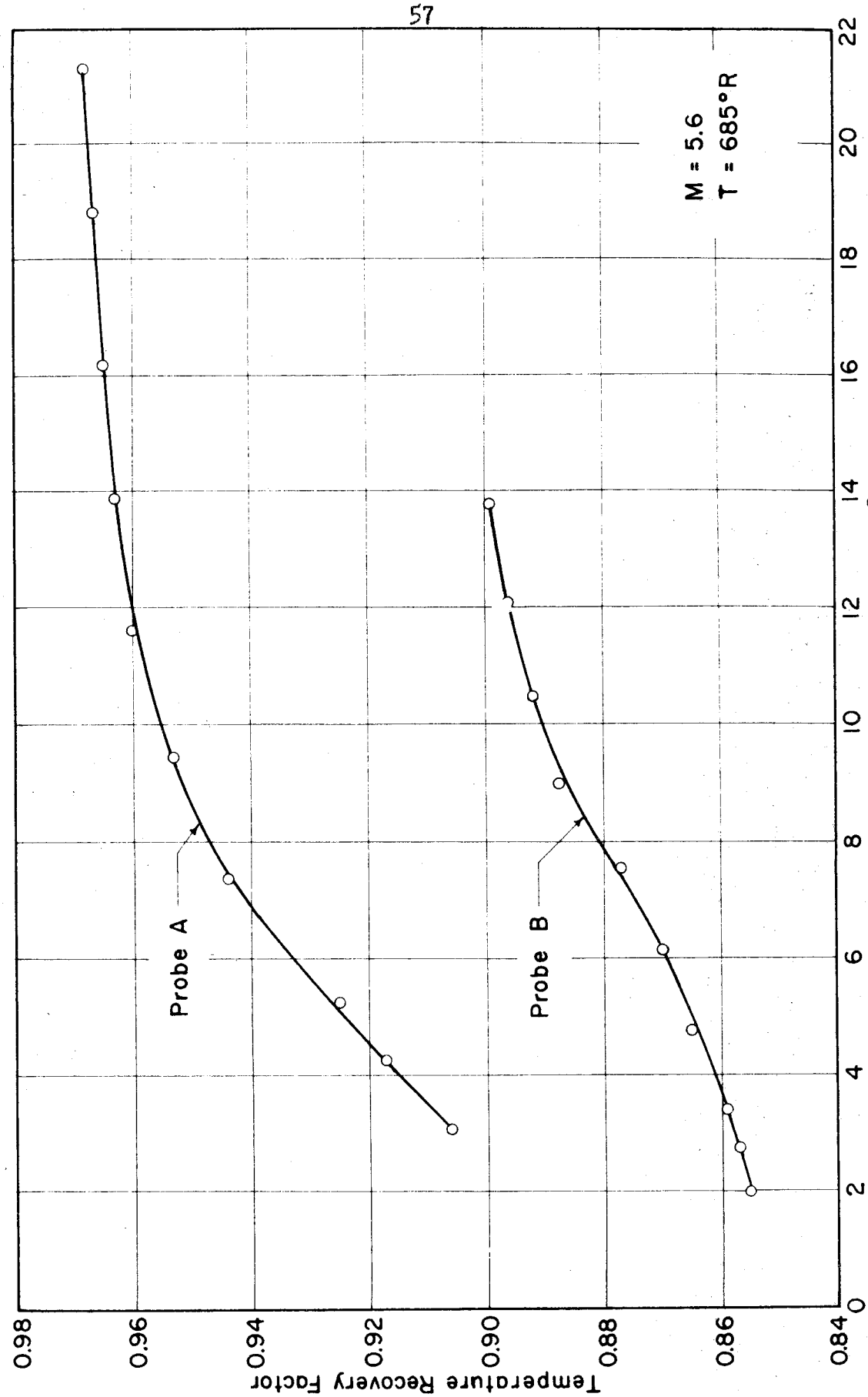

COMPARATIVE RECOVERY FACTORS FOR TWO TEMPERATURE PROBES

FIG. 17

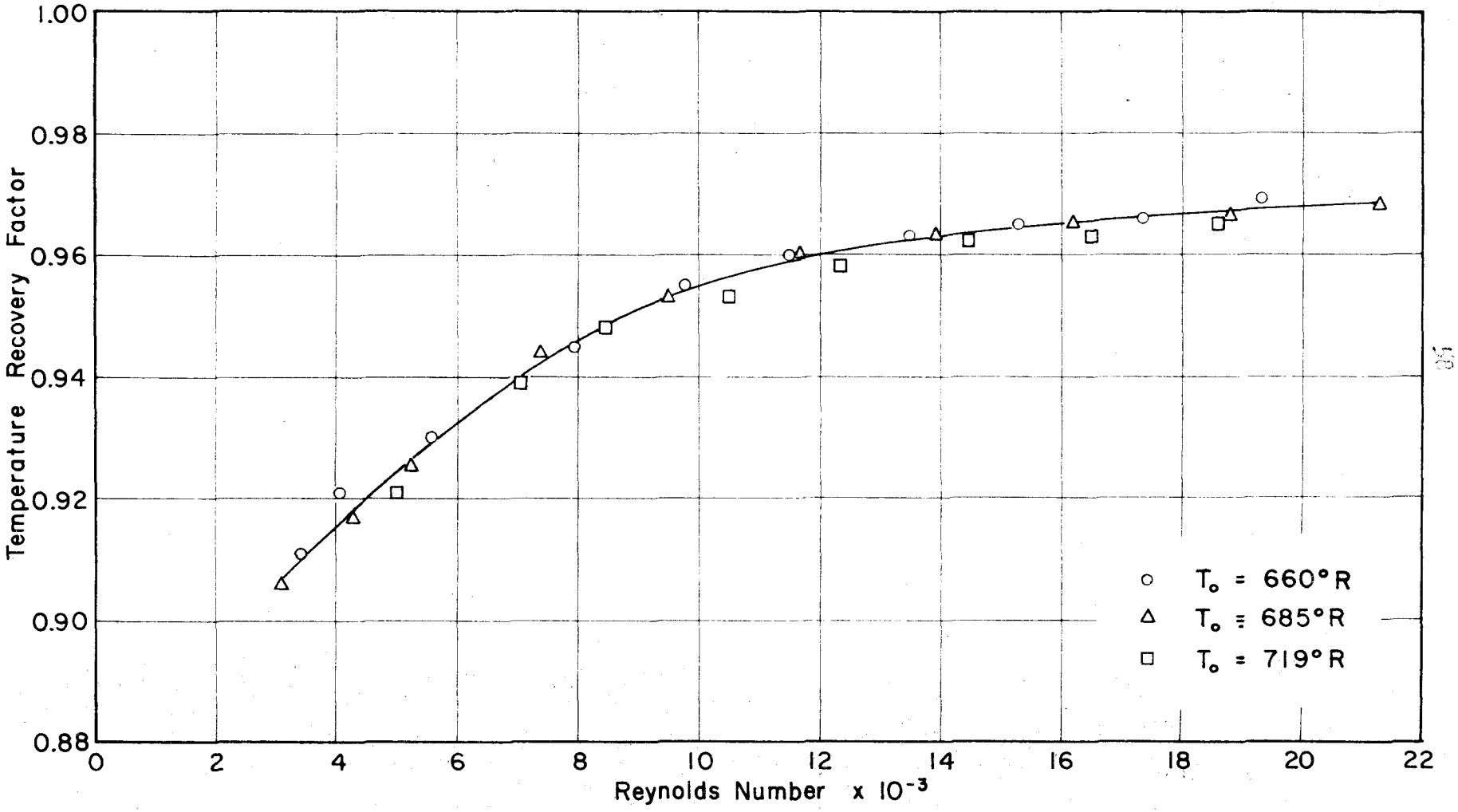

VARIATION OF RECOVERY FACTOR WITH REYNOLDS NUMBER FOR PROBE A

FIG. 18

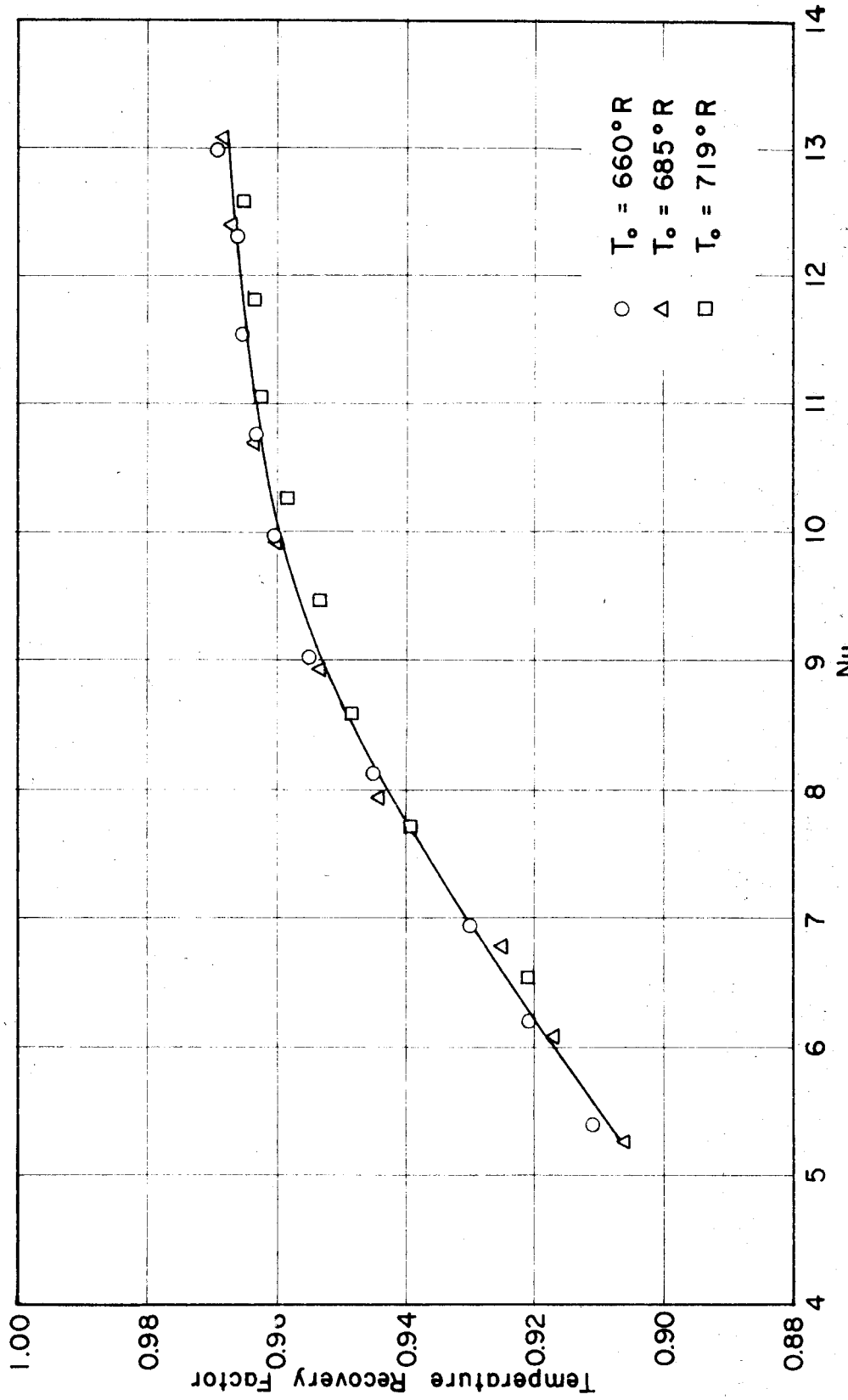

VARIATION OF RECOVERY FACTOR WITH NUSSELT NUMBER FOR PROBE A

FIG. 19

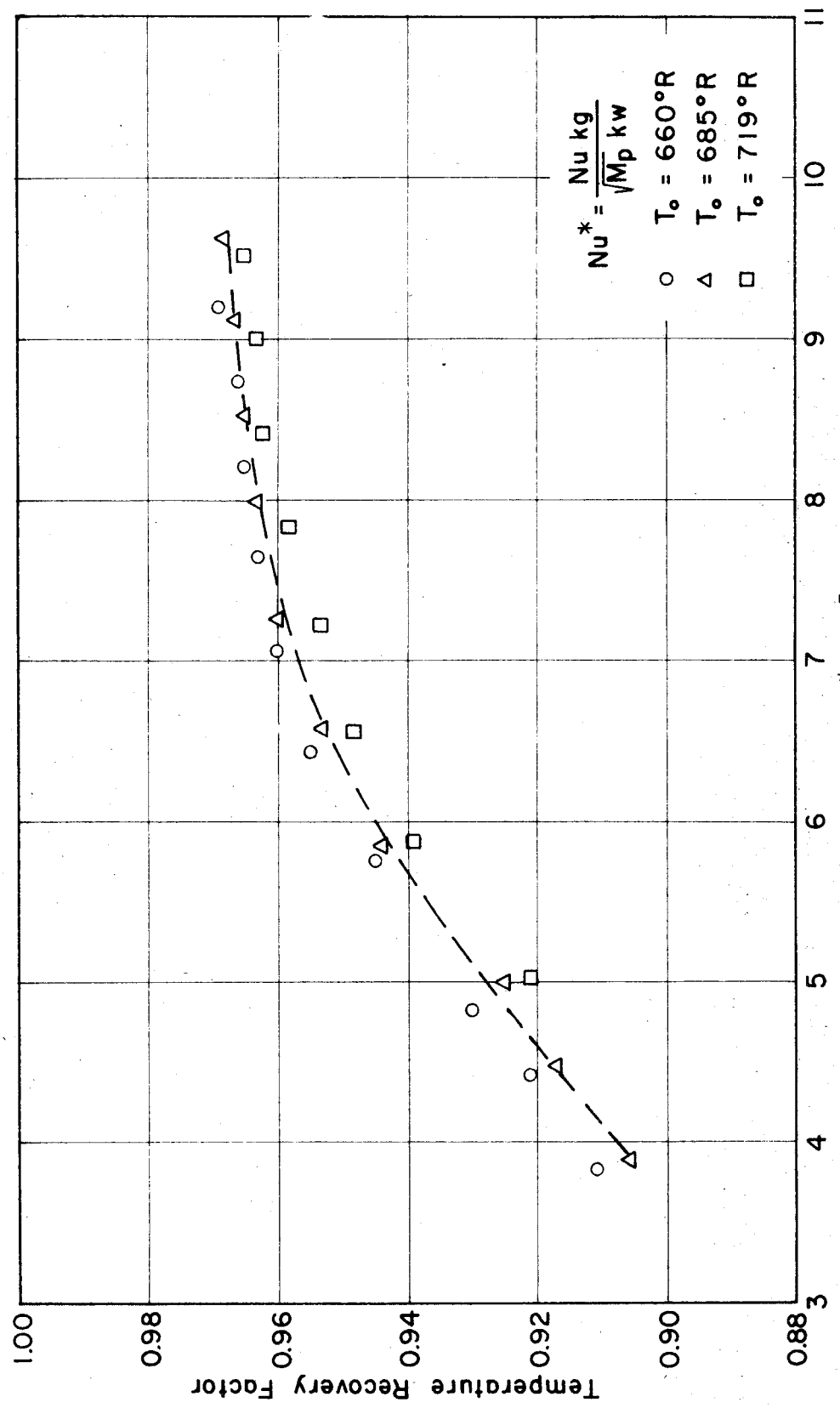

VARIATION OF RECOVERY FACTOR WITH Nu^* FOR PROBE A

FIG. 20